



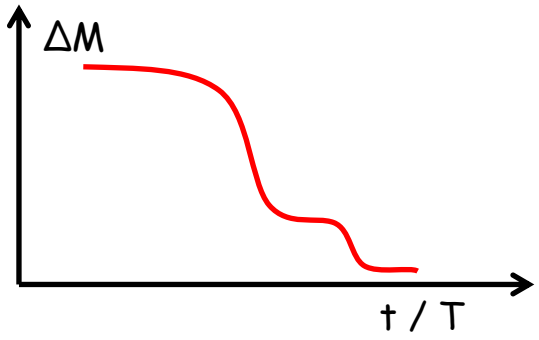
Operando thermal analysis

Andrey Tarasov
8.12.2017

Definition of TA

Group of physical-chemical methods which deal with studying materials and processes under conditions of programmed changing's of the surrounding temperature.

Thermogravimetry

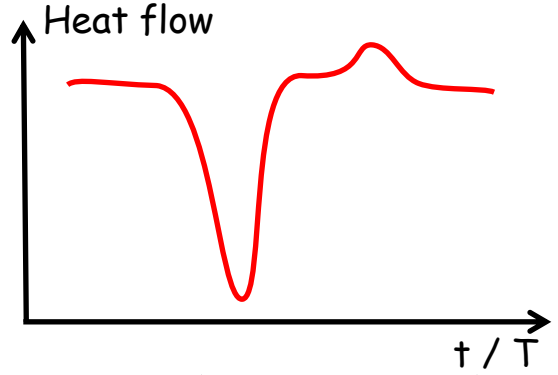


$$r \equiv \frac{dN}{d\tau} = \frac{1}{M} \cdot \frac{dm}{d\tau}$$

$$\Delta m = M \cdot \Delta N$$



Differential Scanning Calorimetry



$$\phi \equiv \frac{dQ}{d\tau} = m \cdot C_p \cdot \frac{dT}{d\tau}$$

$$\Delta Q = m \cdot C_p \cdot \Delta T$$



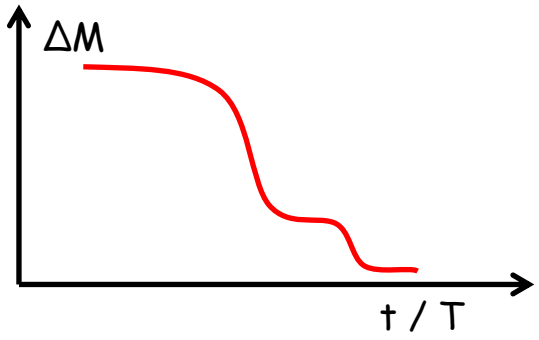
Key parameters:

Course of the reaction, yield of the reaction Enthalpy of formation/transformation (reaction, phase transition)

Definition of TA

Group of physical-chemical methods which deal with studying materials and processes under conditions of programmed changing's of the surrounding temperature.

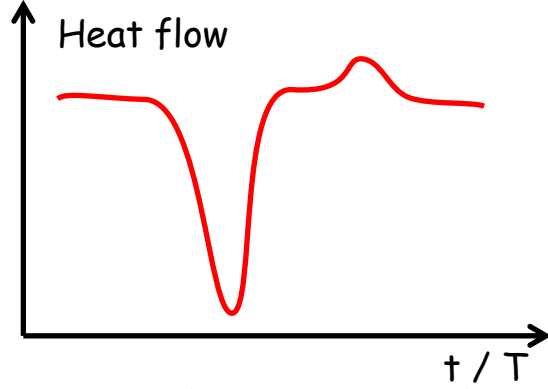
Thermogravimetry



$$r \equiv \frac{dN}{d\tau} = \frac{1}{M} \cdot \frac{dm}{d\tau}$$

$$\Delta m = M \cdot \Delta N$$

Differential Scanning Calorimetry

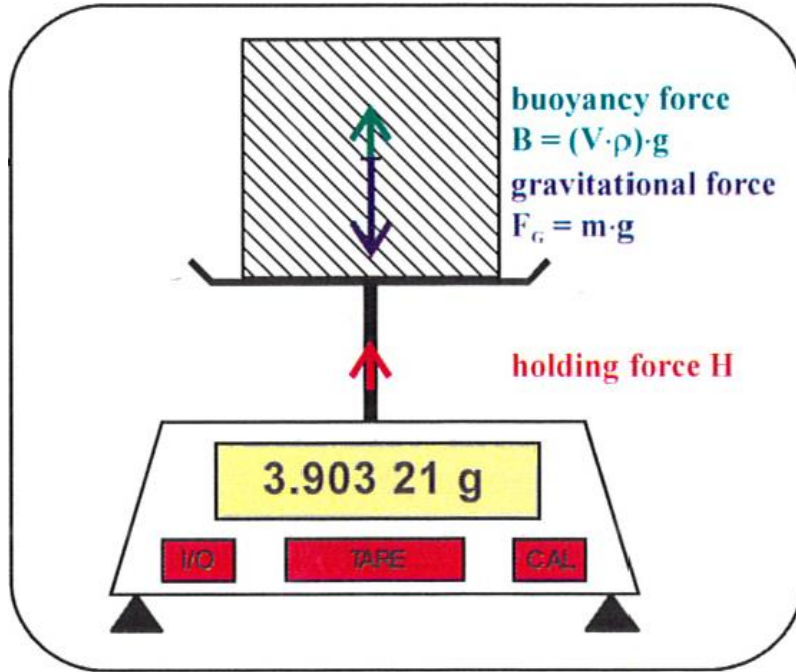


$$\phi \equiv \frac{dQ}{d\tau} = m \cdot C_p \cdot \frac{dT}{d\tau}$$

$$\Delta Q = m \cdot C_p \cdot \Delta T$$

operando ≈ in-situ – „on site“ → in heterogeneous catalysis
 „in reaction mixture under operation conditions“

T, P, μ → conversion/activity, mass – transfer conditions



S_{MP} - Measurement signal

F_B - Buoyancy force, $f(T)$

m_A - Mass of adsorbed gas, $f(T)$

m_{SC} - Mass of sample container

m_S - Mass of sample, $f(T)$

V_A - Volume of adsorbed gas, $f(T)$

V_{SC} - Volume of sample container

V_S - Volume of sample, $f(T)$

ρ_{gas} - Density of gas, $f(T)$

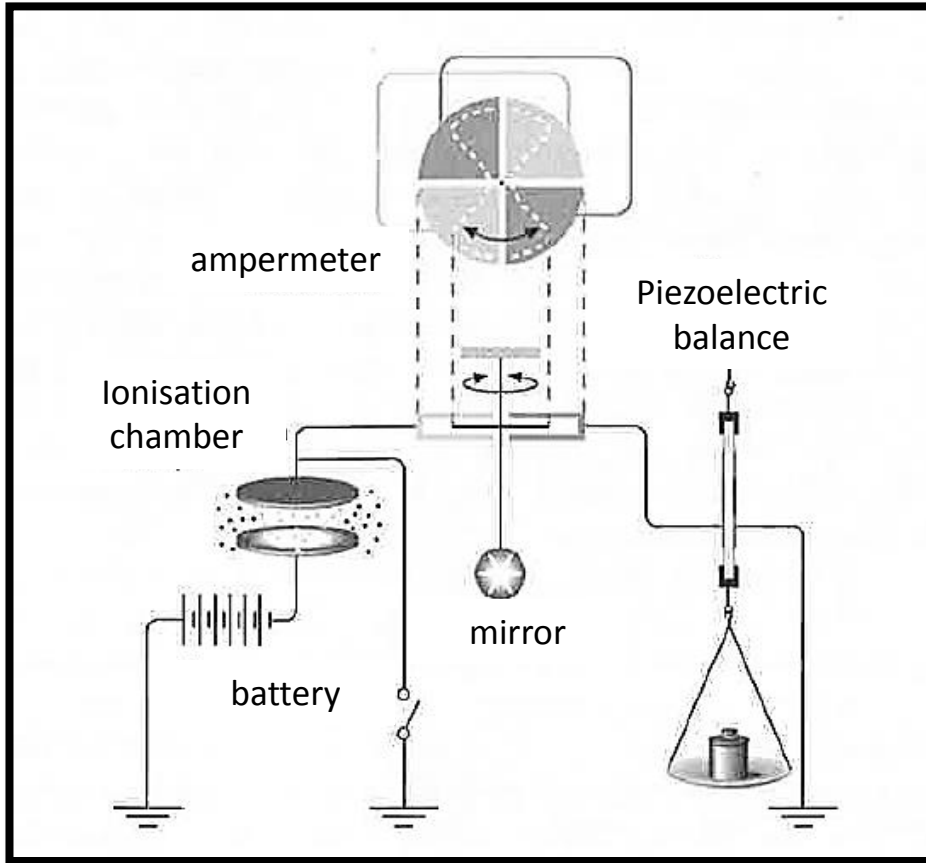
$$S_{MP} \cdot g = ((m_{SC} + m_S + m_A) - (V_{SC} + V_S + V_A) \cdot \rho_{gas}) \cdot g$$

Signal

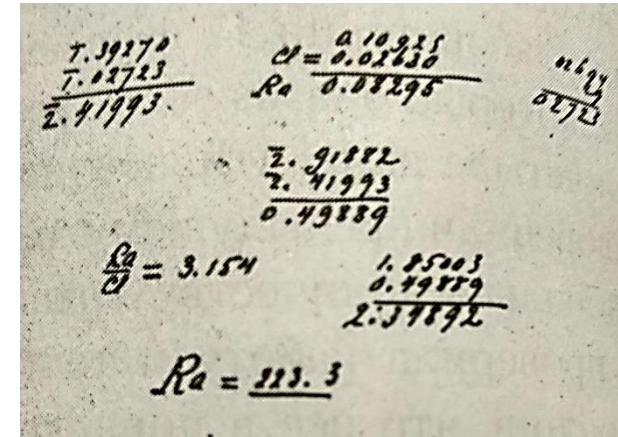
System mass

Buoyancy Force

1898, Marie Curie “weighted” radioactivity



^{88}Ra , ^{84}Po

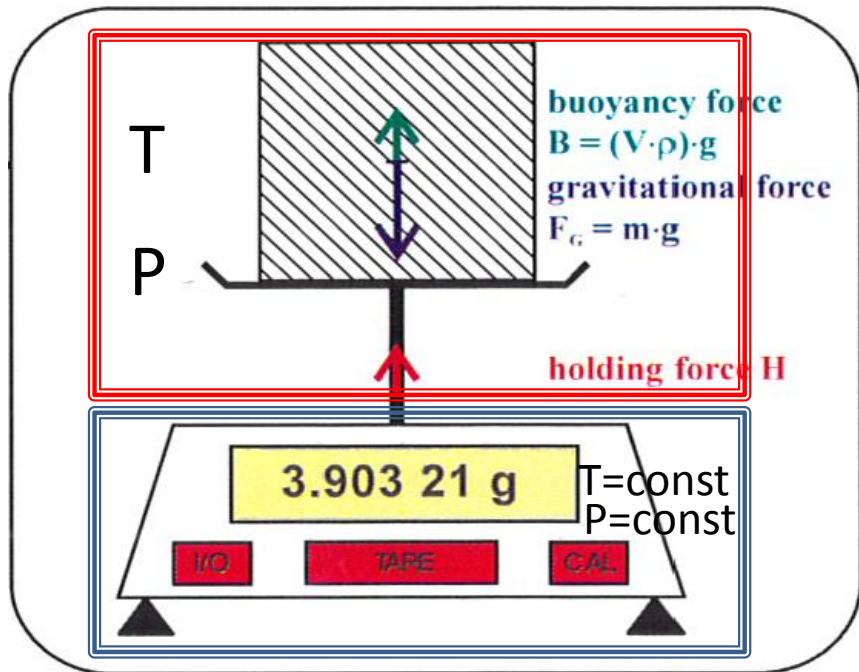


Marie and Pierre Curies diary, 1902. Curie Museum

$Mr(\text{Ra}) = 225$

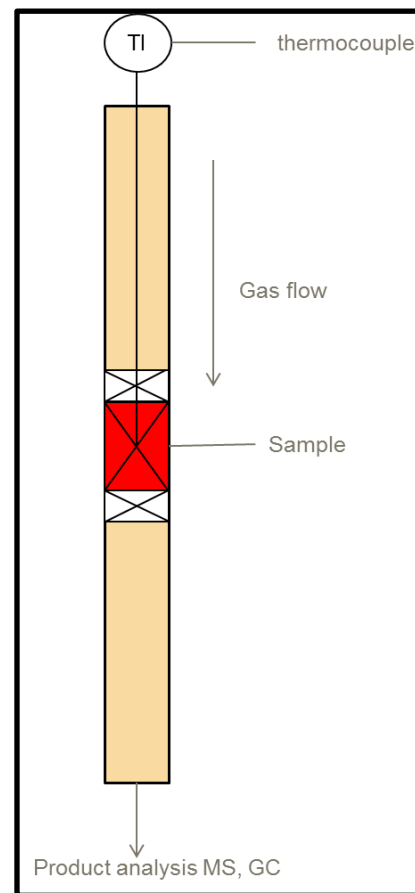
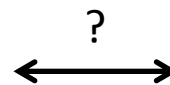


1 g earth crust $\approx 10^{-13}$ g Ra

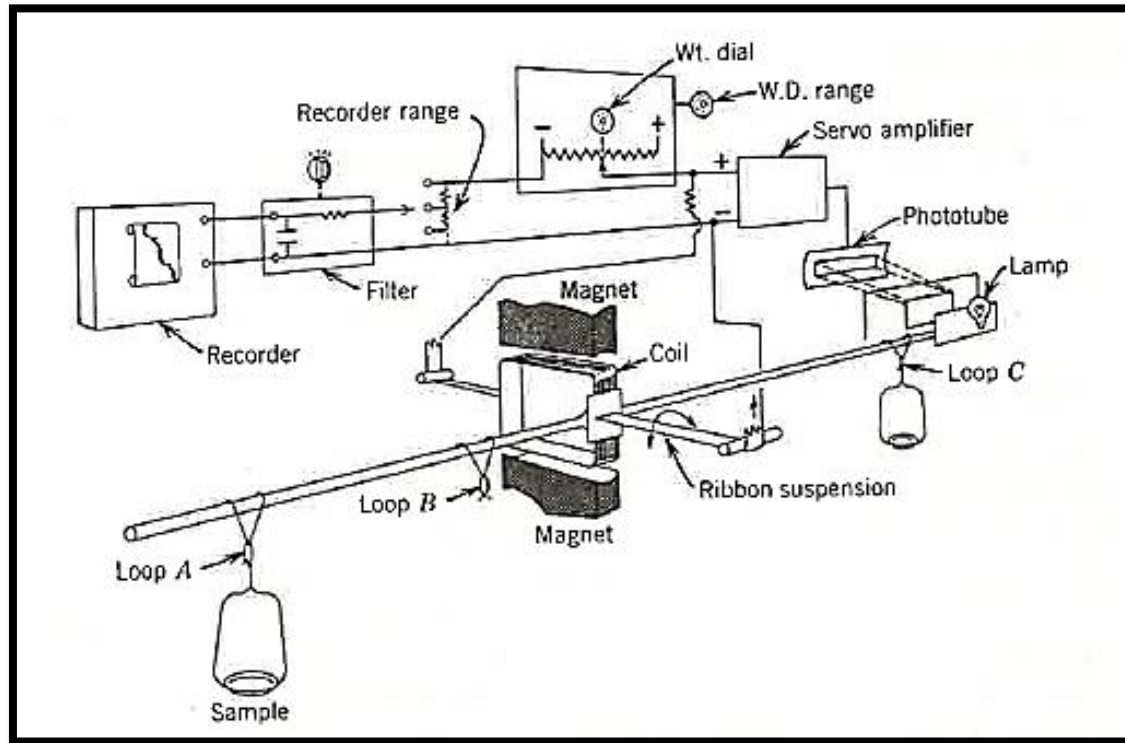


$$S_{MP} \cdot g = ((m_{SC} + m_S + m_A) - (V_{SC} + V_S + V_A) \cdot \rho_{gas}) \cdot g$$

Signal System mass Buoyancy Force

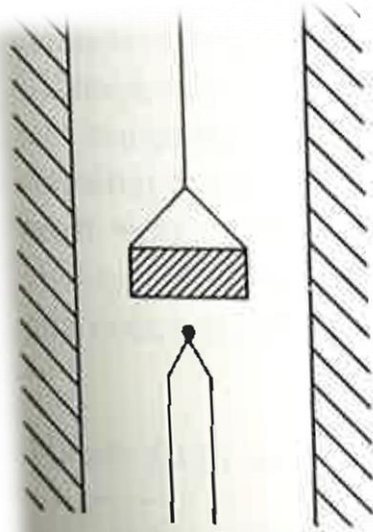


- S_{MP} - Measurement signal
- F_B - Buoyancy force, $f(T)$
- m_A - Mass of adsorbed gas, $f(T)$
- m_{SC} - Mass of sample container
- m_S - Mass of sample, $f(T)$
- V_A - Volume of adsorbed gas, $f(T)$
- V_{SC} - Volume of sample container
- V_S - Volume of sample, $f(T)$
- ρ_{gas} - Density of gas, $f(T)$

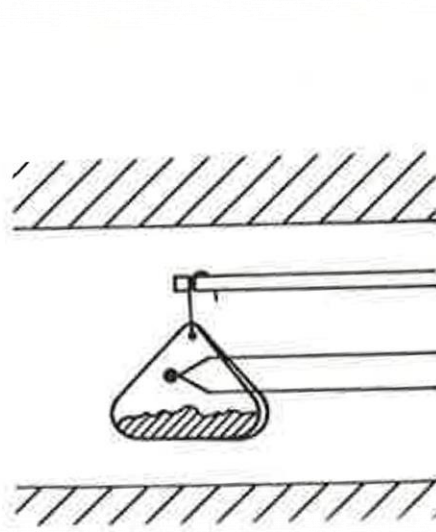


Schematic diagram of the Cahn Electrobalance

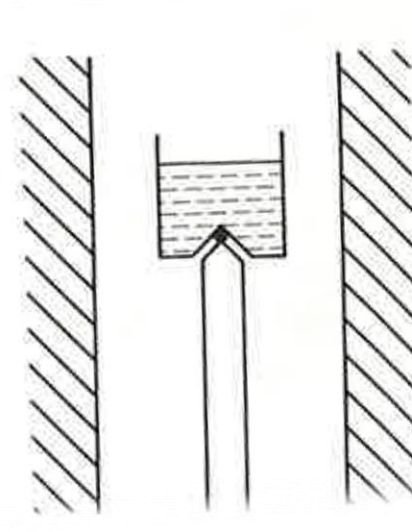
Commercially available thermobalances employ one of the Cahn-type electromagnetic balance



No contact



Close proximity



With contact



TGA type S sample carrier with different crucibles and plates, TGA type W sample carrier (W3%Re/W25%Re); for more crucibles and plates, see TGA crucibles table.

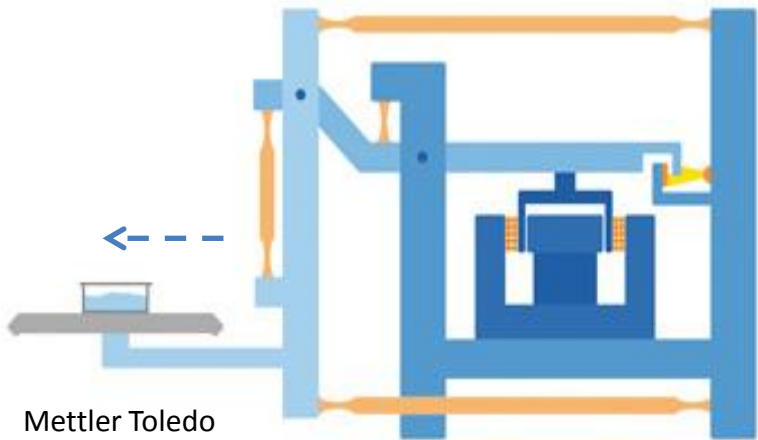


TGA-DTA sensor for hanging samples

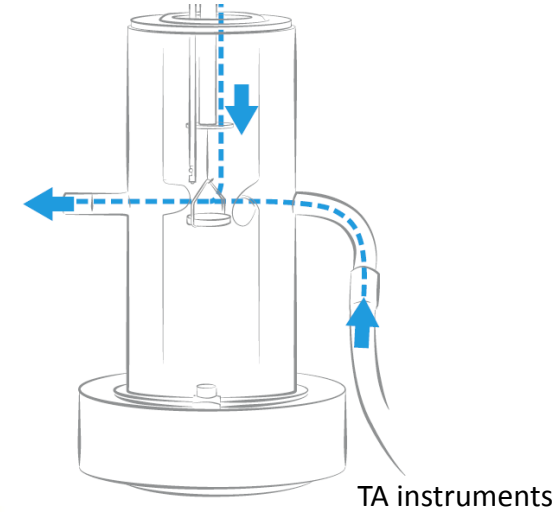
TGA sample carrier for hanging samples



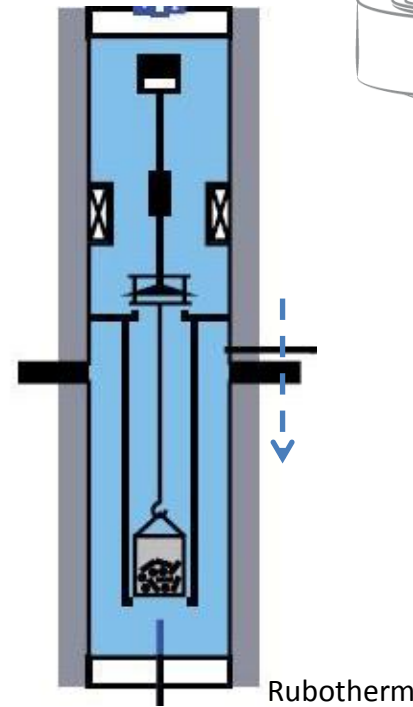
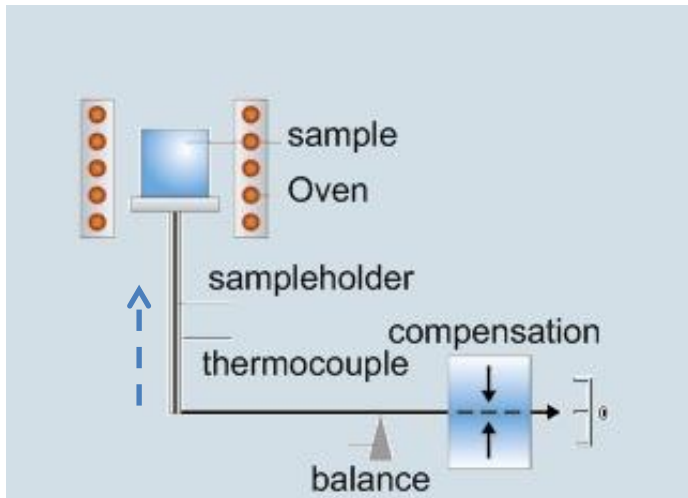
Horizontal, parallel-guided



Vertical, free suspended

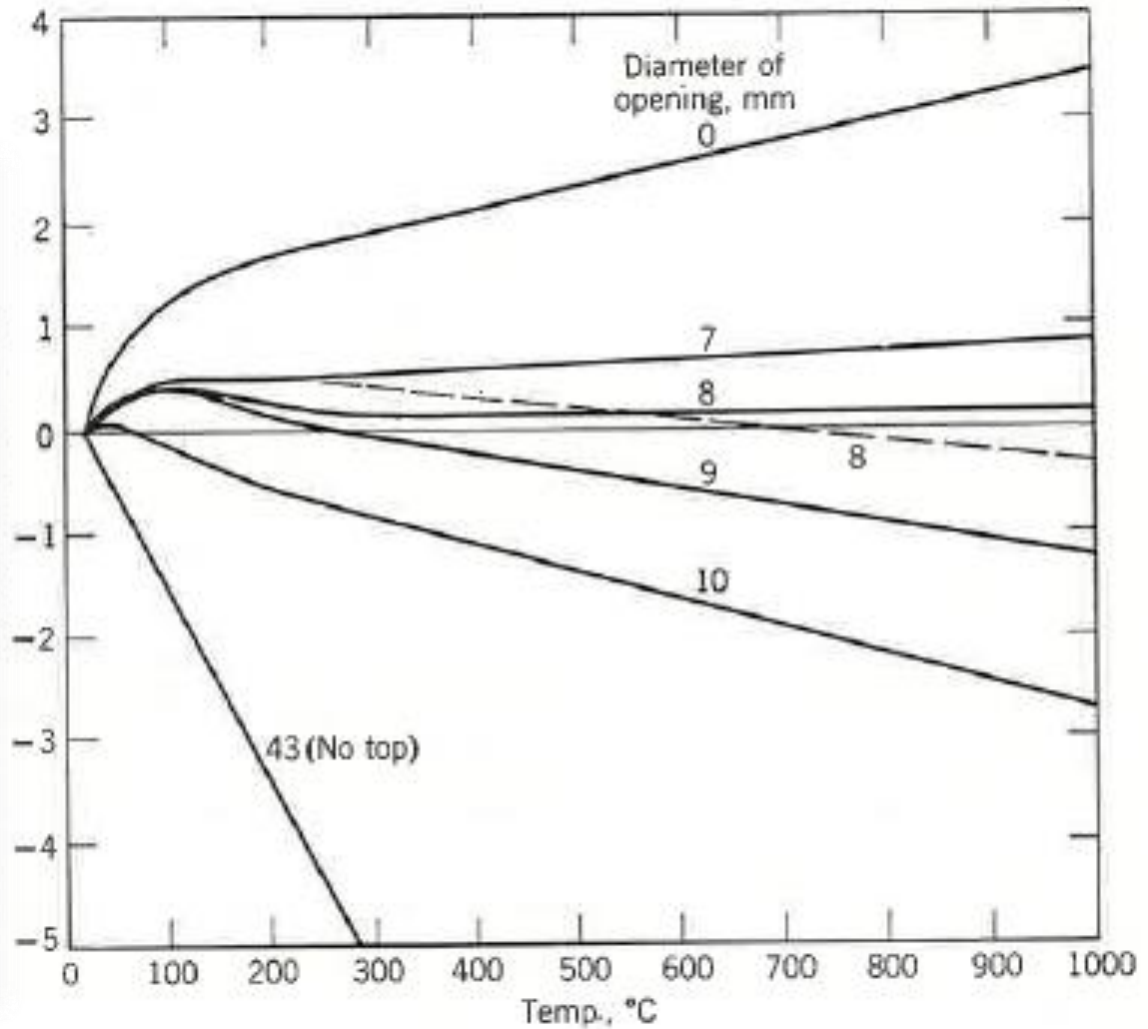
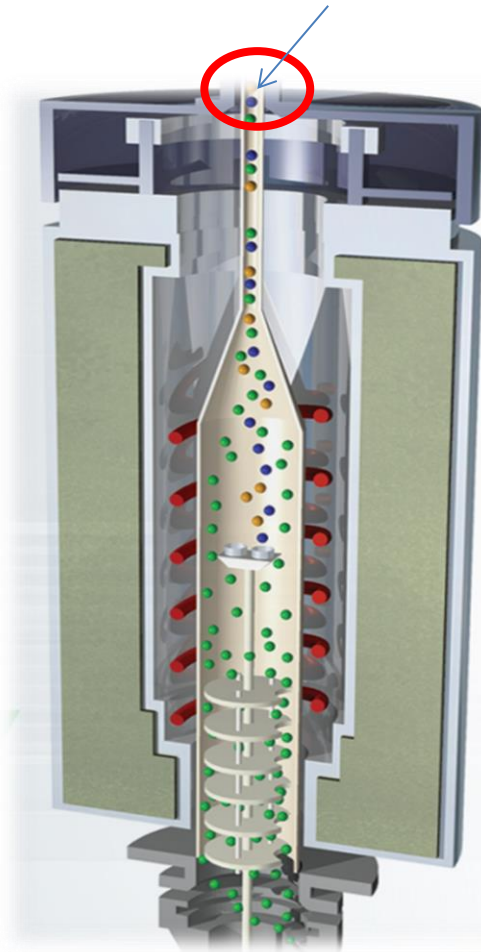


Vertical, top-loader

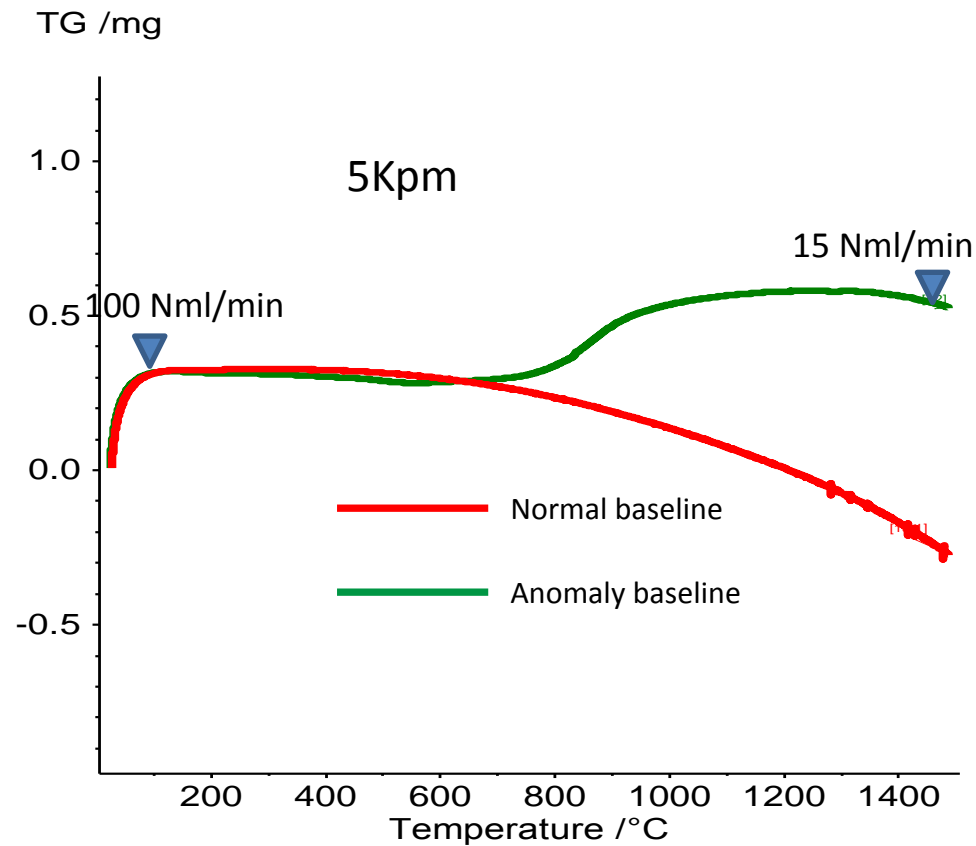


Netzsch, Setaram

Rubotherm



Effect of furnace top opening on apparent mass-change, 5Kpm



- Reproducible in different gas atmospheres and by different heating rates

gas flow decreases during the heating, starting from 600°C



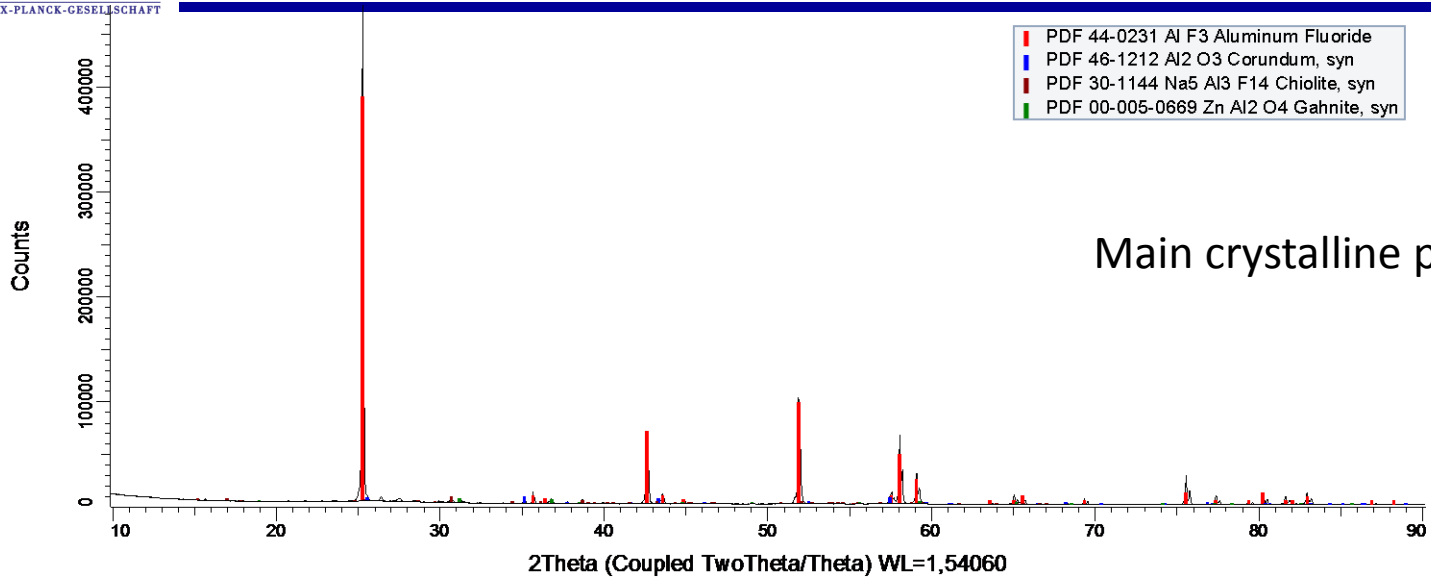
Reassembling the oven

Top part of the tube was plugged with solid material

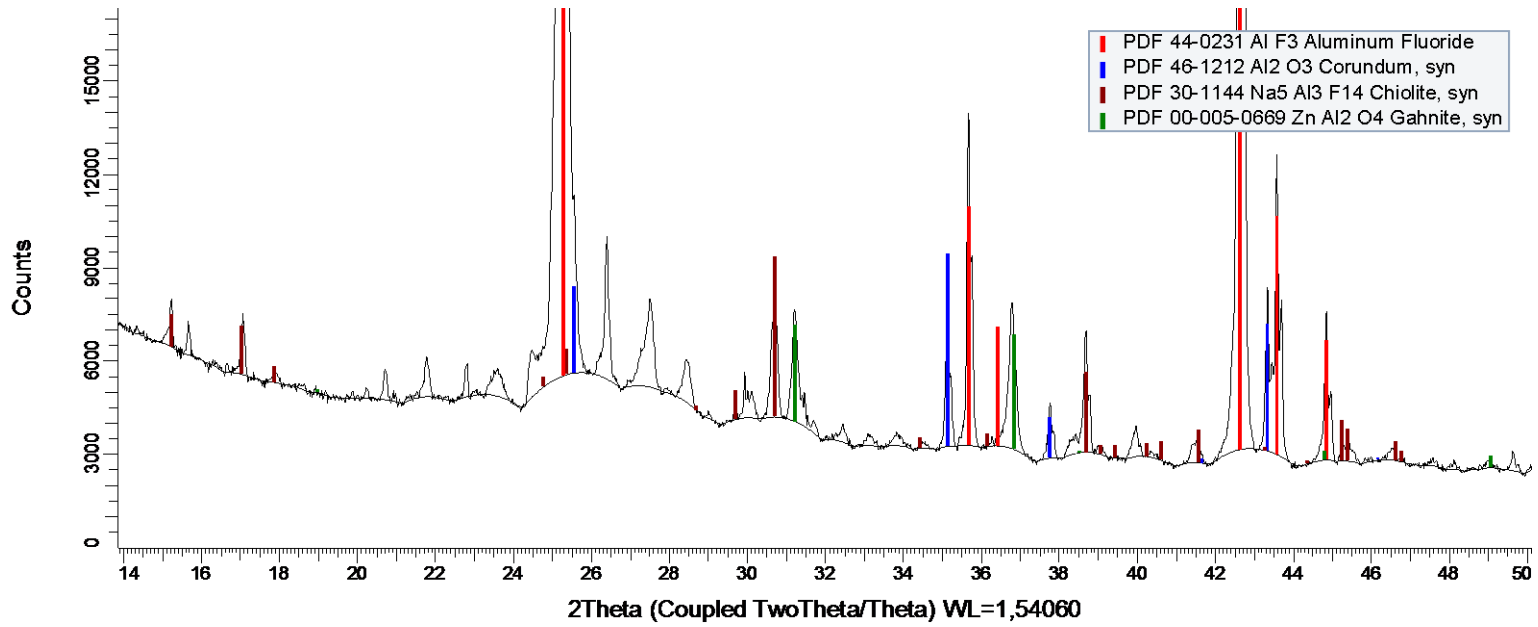
The material was analyzed by various techniques



- PDF 44-0231 Al F3 Aluminum Fluoride
- PDF 46-1212 Al2 O3 Corundum, syn
- PDF 30-1144 Na5 Al3 F14 Chiolite, syn
- PDF 00-005-0669 Zn Al2 O4 Gahnite, syn



Main crystalline phase is AlF_3

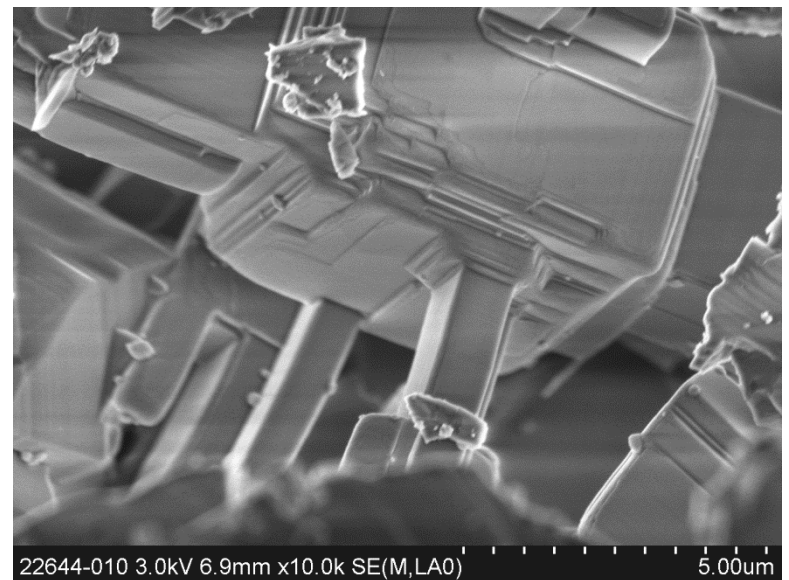
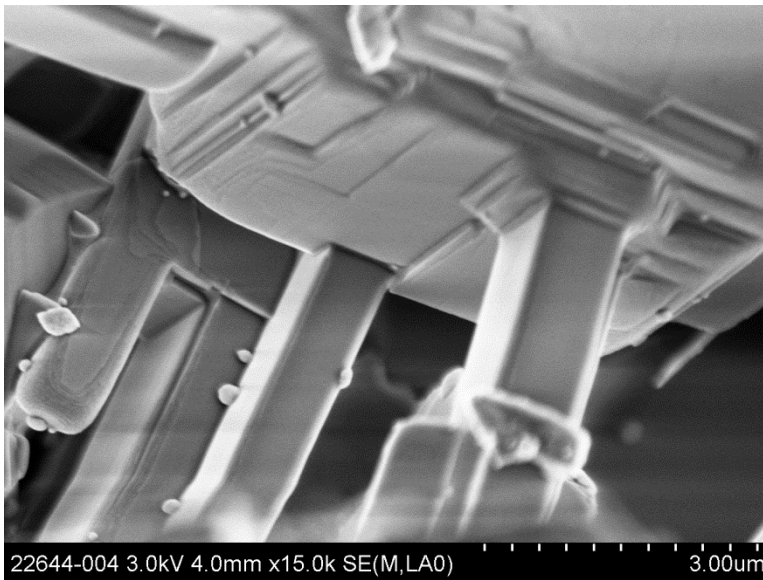
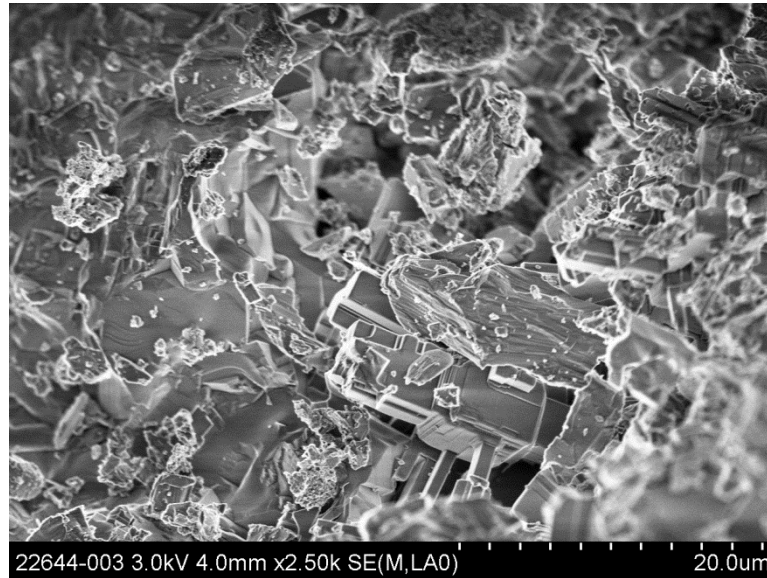


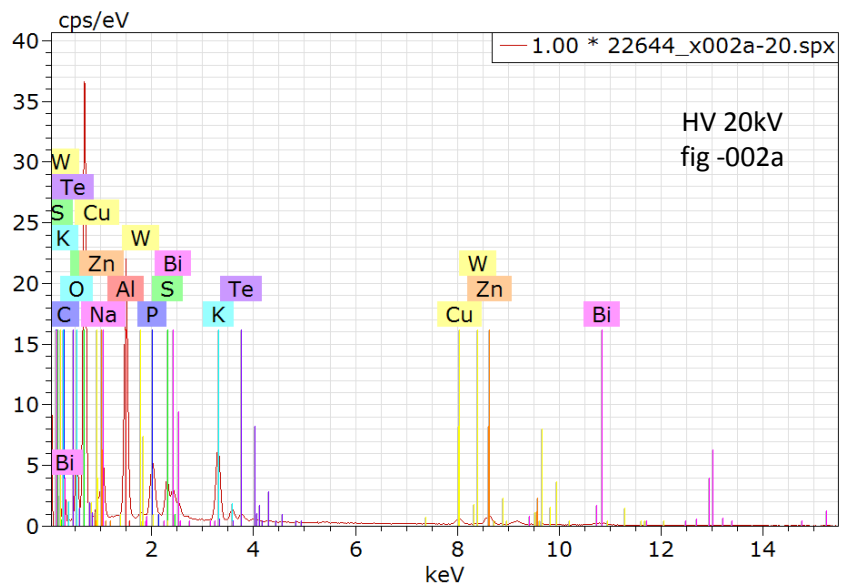
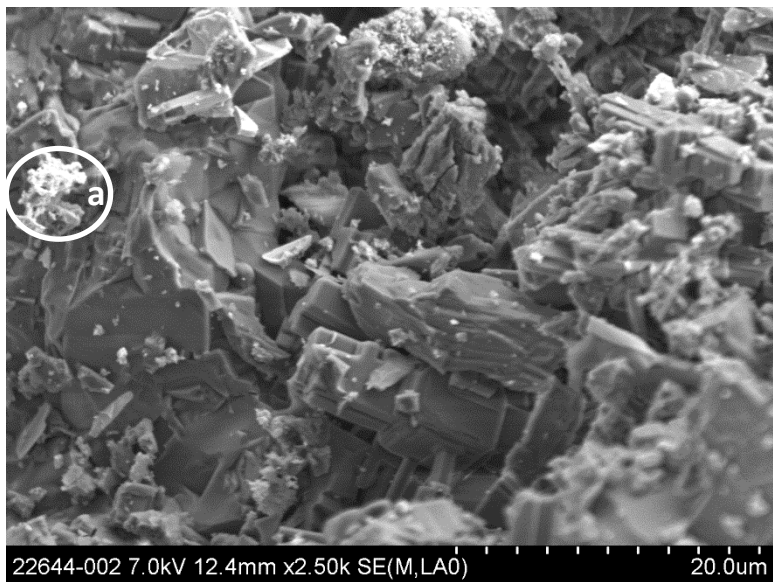
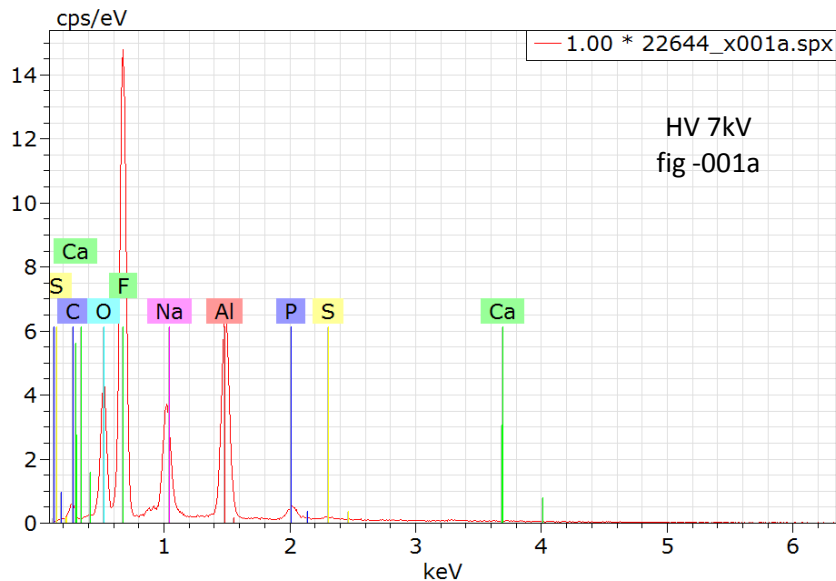
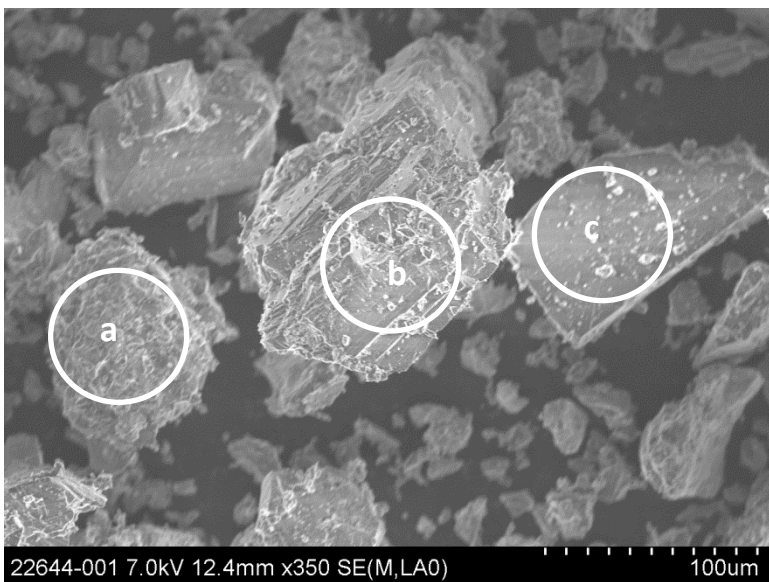
- PDF 44-0231 Al F3 Aluminum Fluoride
- PDF 46-1212 Al2 O3 Corundum, syn
- PDF 30-1144 Na5 Al3 F14 Chiolite, syn
- PDF 00-005-0669 Zn Al2 O4 Gahnite, syn

Formula	Concentration, %
AlF3	92.4
Bi2O3	0.45
CaO	0.62
Cr2O3	0.54
CuO	1.17
Fe2O3	1.69
K2O	0.55
MoO3	2.95
NiO	0.16
P2O5	0.33
Ru	0.642
SiO2	1.3
SO3	0.45
WO3	0.33
ZnO	2.21

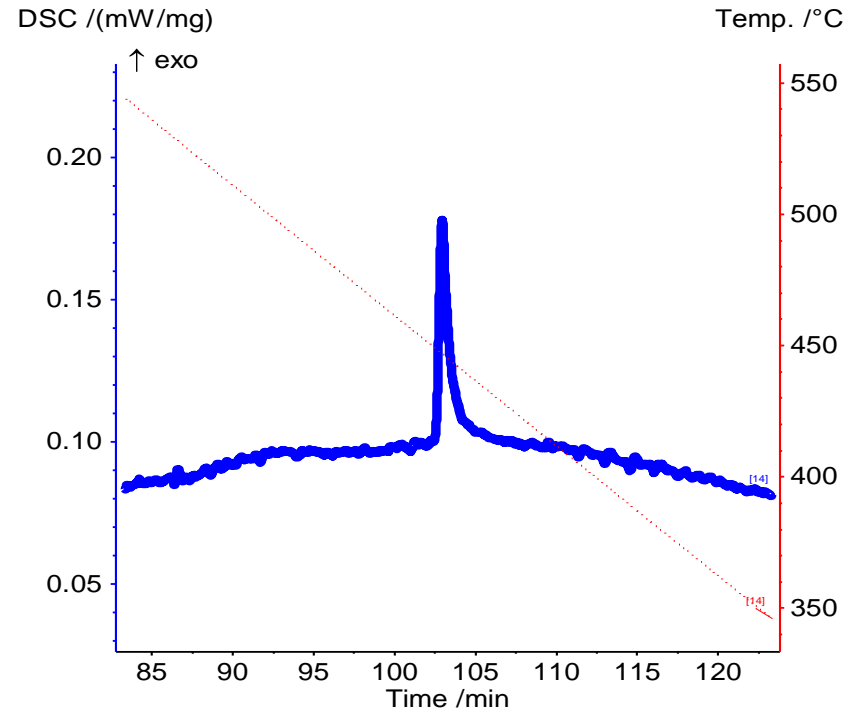
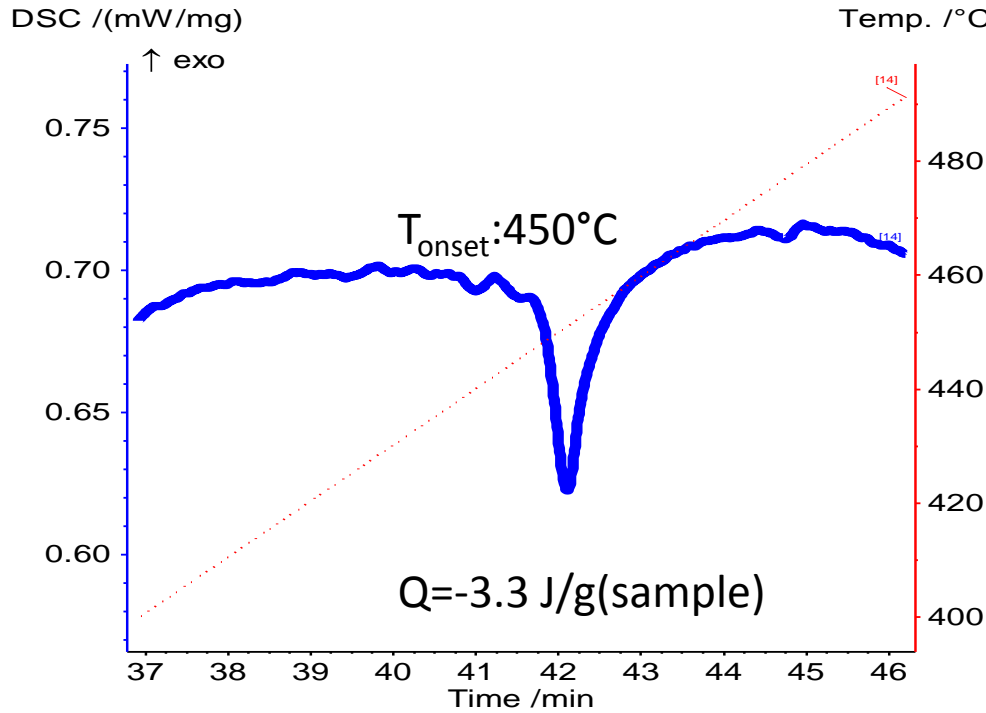
Elemental analysis

Surface microstructure





- Reversible melting point (explains dynamic behaviour of the flow)



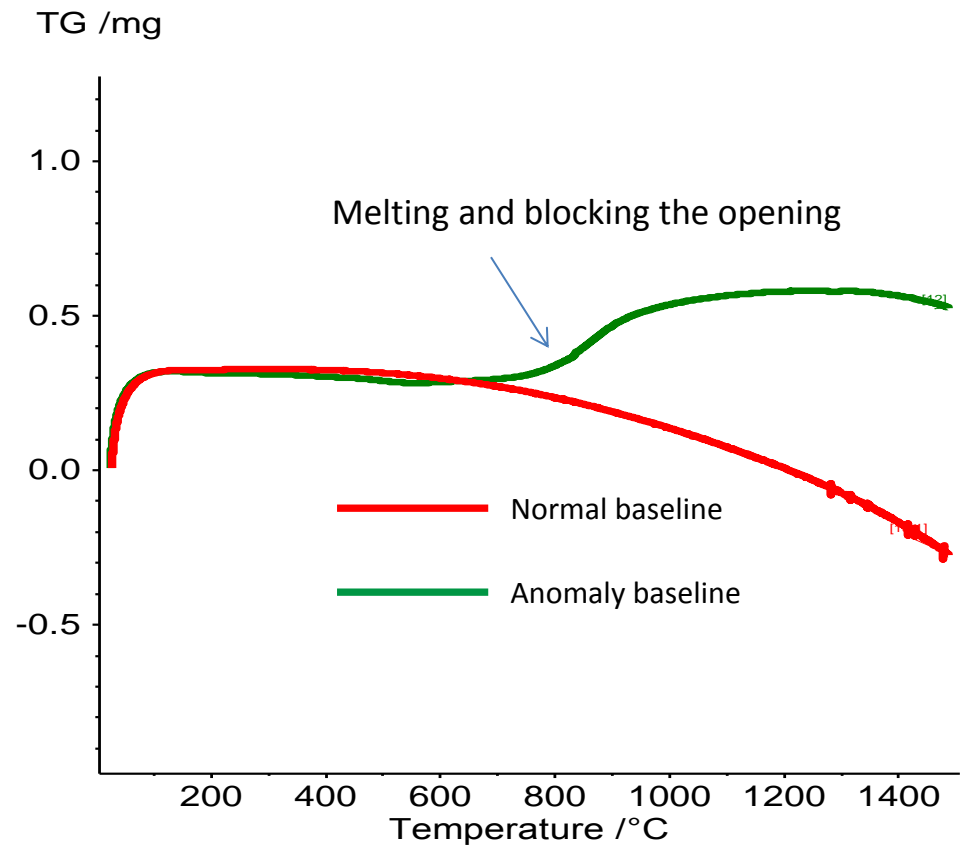
eutectic LiF-NaF-KF (46.5-11.5-42) $T_m = 454^\circ\text{C}$

AgF $T_m = 435^\circ\text{C}$

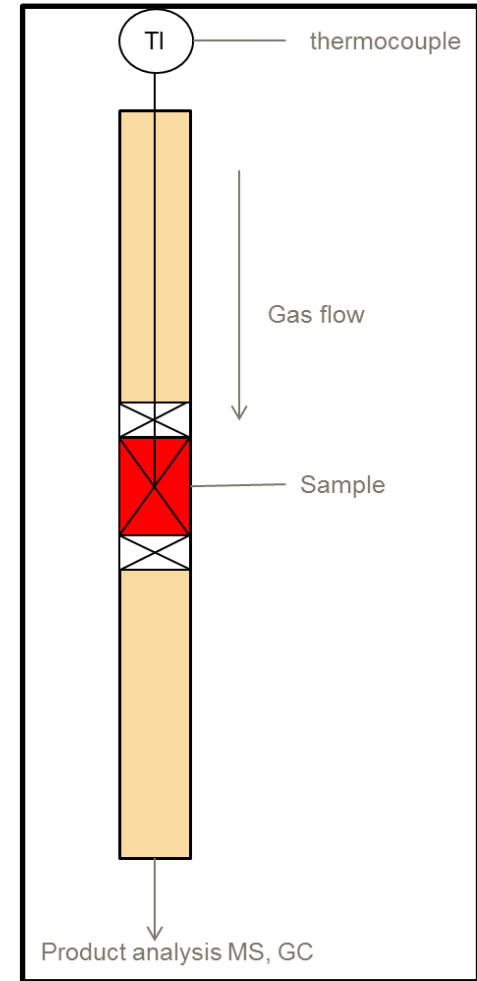
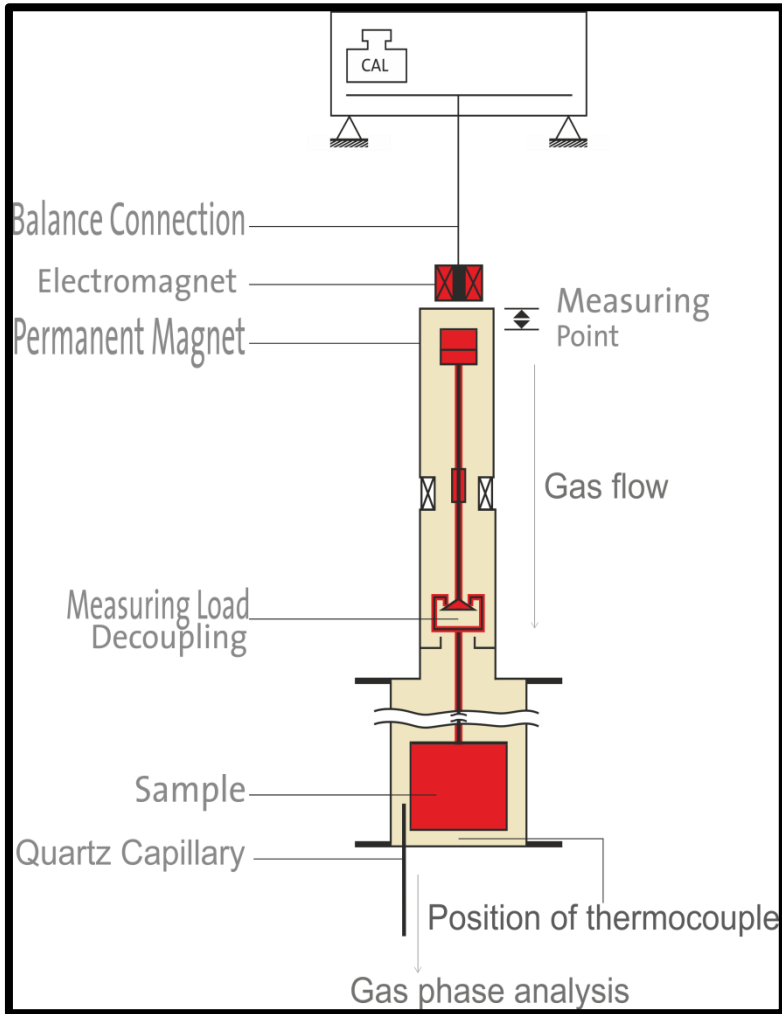
$\text{K}_{1-3}\text{AlF}_{4-6}$, CsAlF_4 (NOCOLOK[®]) $T_m = 560-570^\circ\text{C}$

Zn $T_m = 419^\circ\text{C}$

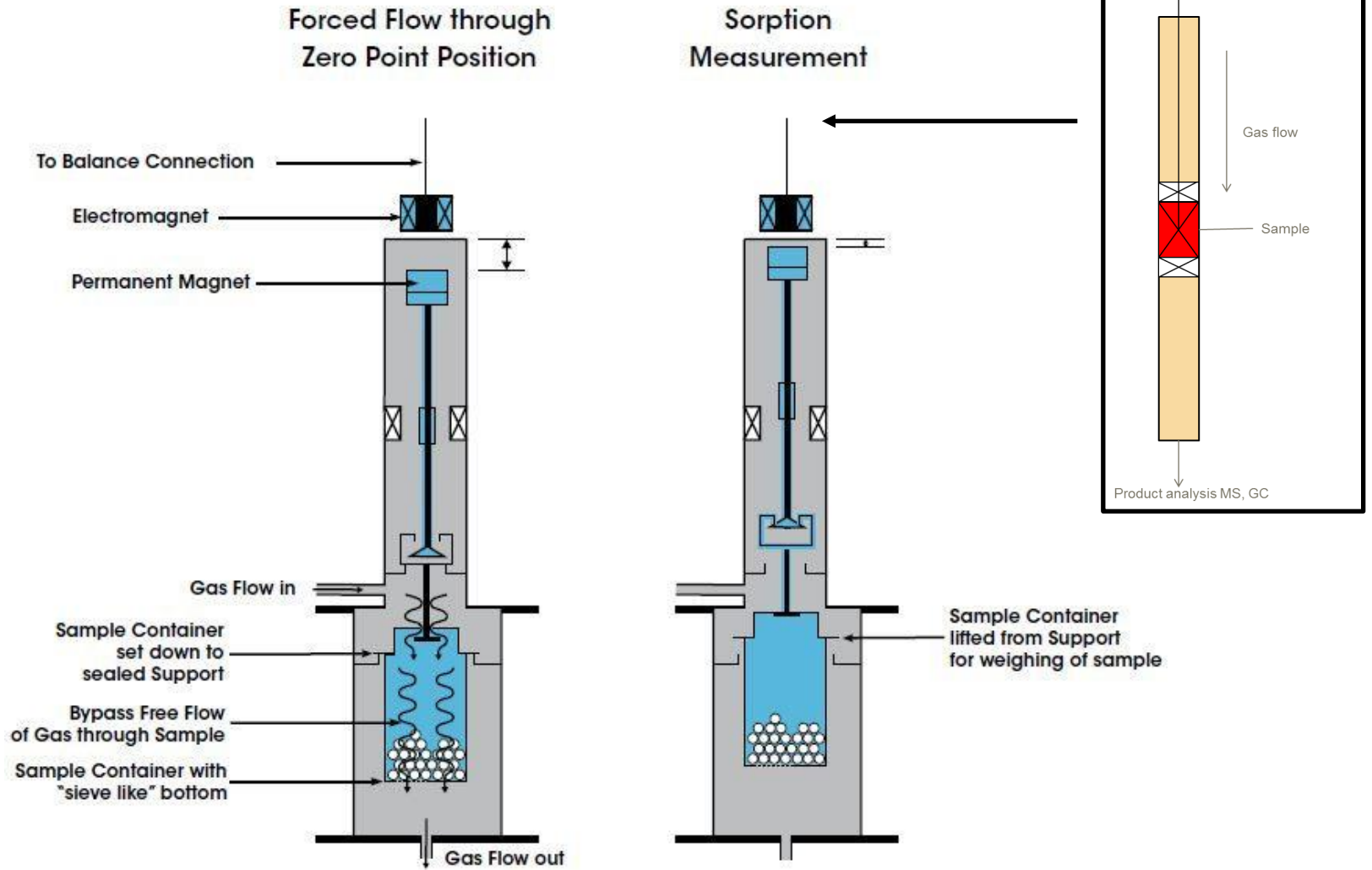
Amount of the phase undergoes melting 1.5-3%

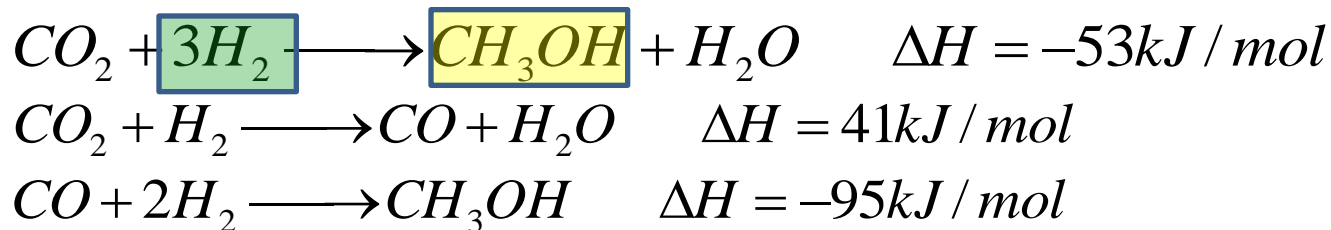
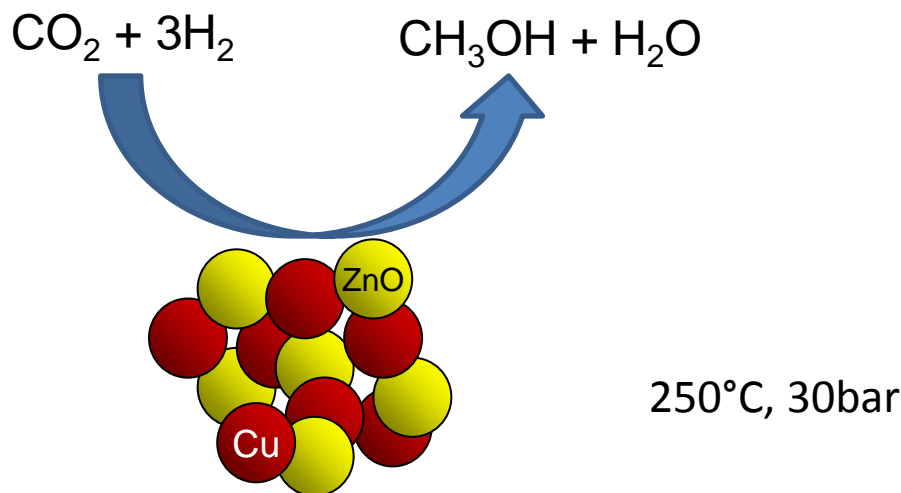


Nearing the plug flow conditions



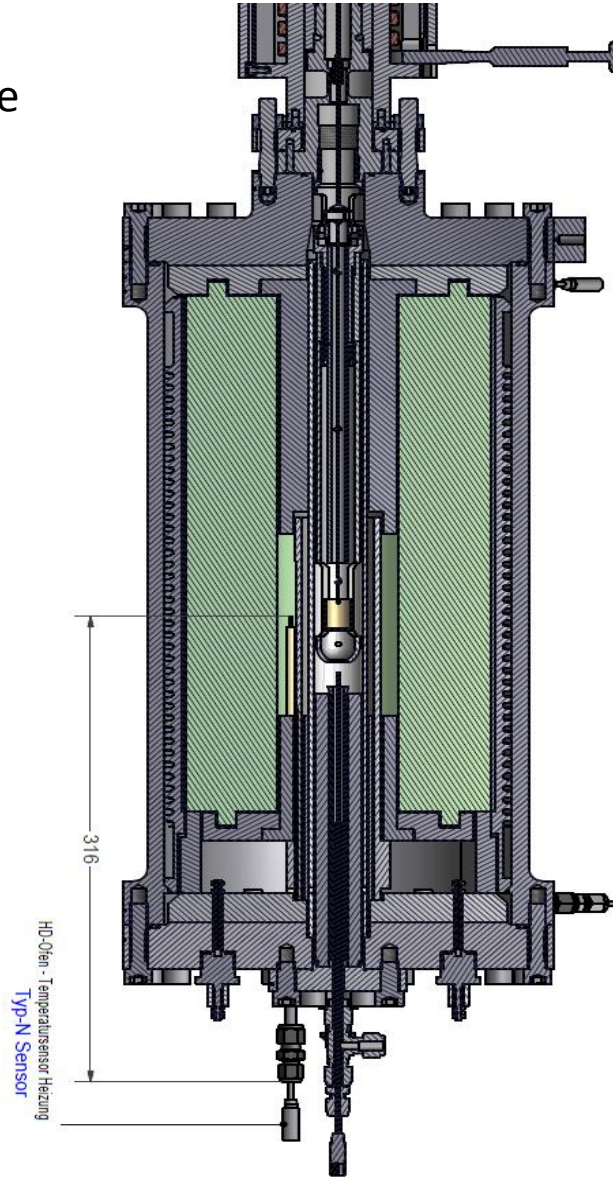
Nearing the plug flow conditions



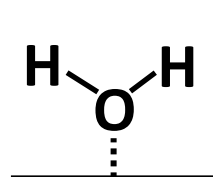


What is the surface composition during the operation?

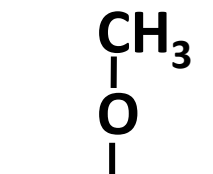
High Pressure Thermobalance



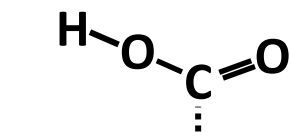
Reaction intermediates and spectators:



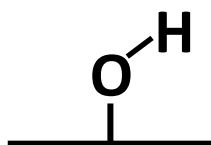
Water



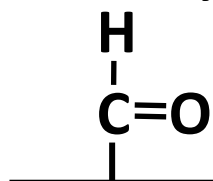
Methoxy



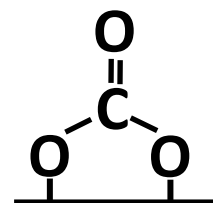
Carboxyl (cis)



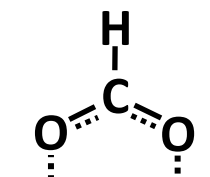
Hydroxy



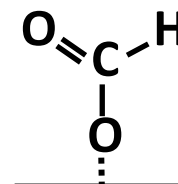
Formyl



Carbonate



Formate (bidentate)

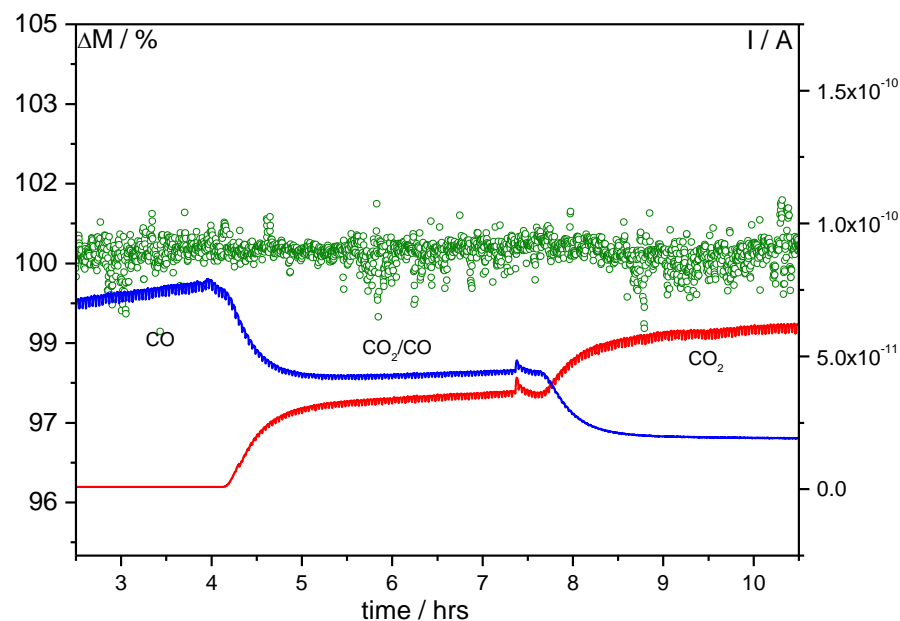


Formate (monodentate)

Case Study: Methanol Synthesis

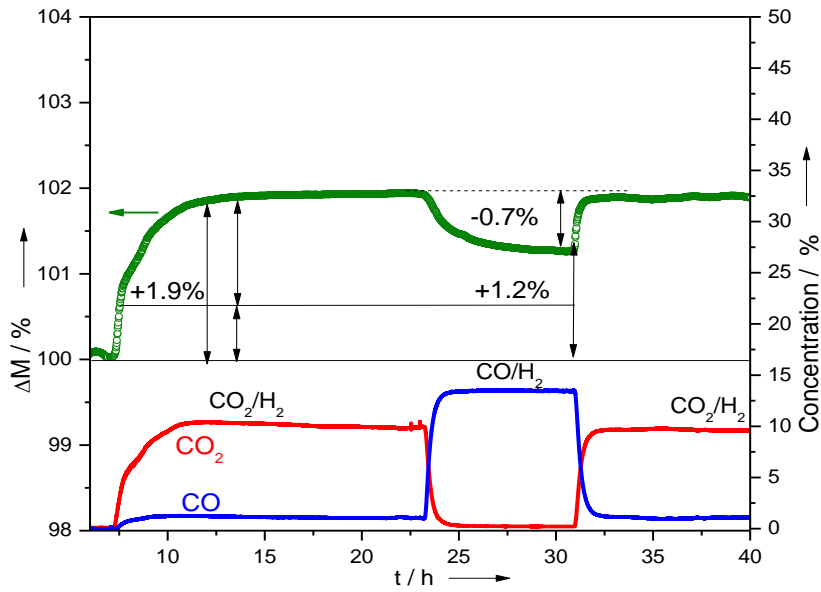
Gas	Density (kg/m ³)
CO/CO ₂ /H ₂ /He(6/8/59/27)	0.33
CO/Ar/H ₂ /He(14/4/59/23)	0.34
CO ₂ /He/H ₂ (12.4/28.8/58.8)	0.35

Density alignment

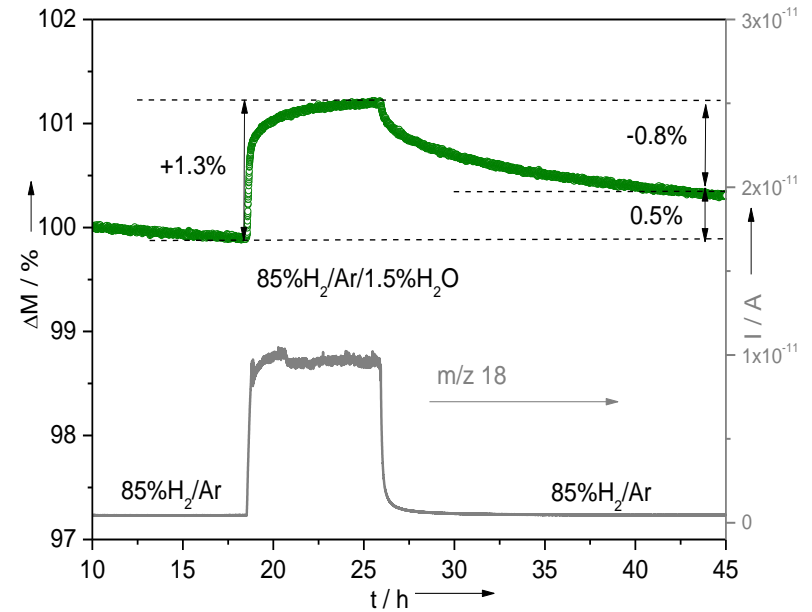


400mg SiO₂, 30 bar, 250°C, feed gas flow 120 ml/min

TG Methanol Synthesis (250°C, 30bar)



Addition of 1.5% H₂O (250°C, 1bar)



Cu sites – 400 $\mu\text{mol g}(\text{cat})^{-1}$

ZnOx sites – 273 $\mu\text{mol g}(\text{cat})^{-1}$

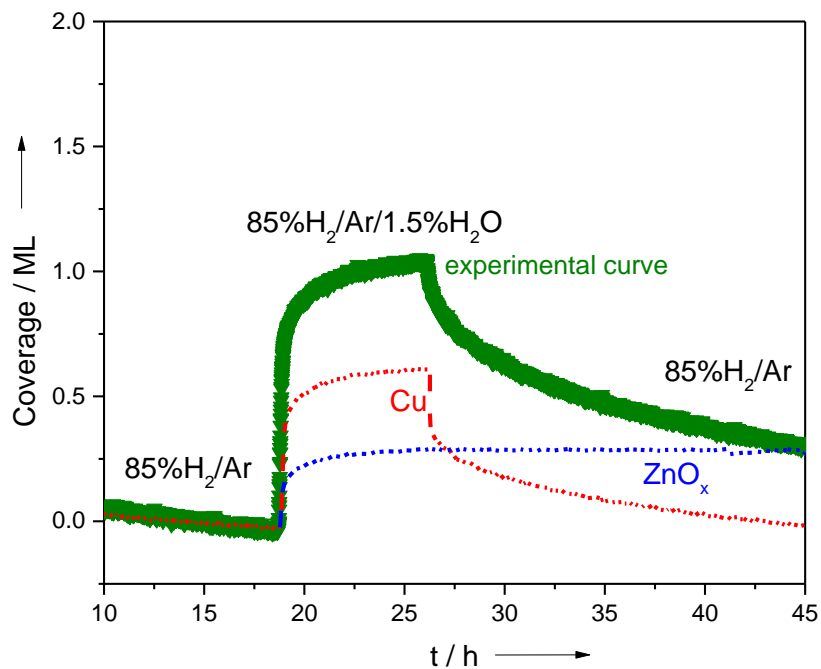
Schumann et al. ACS Catalysis, 2015, 5

Schumann et al. ChemCatChem, 2014, 6

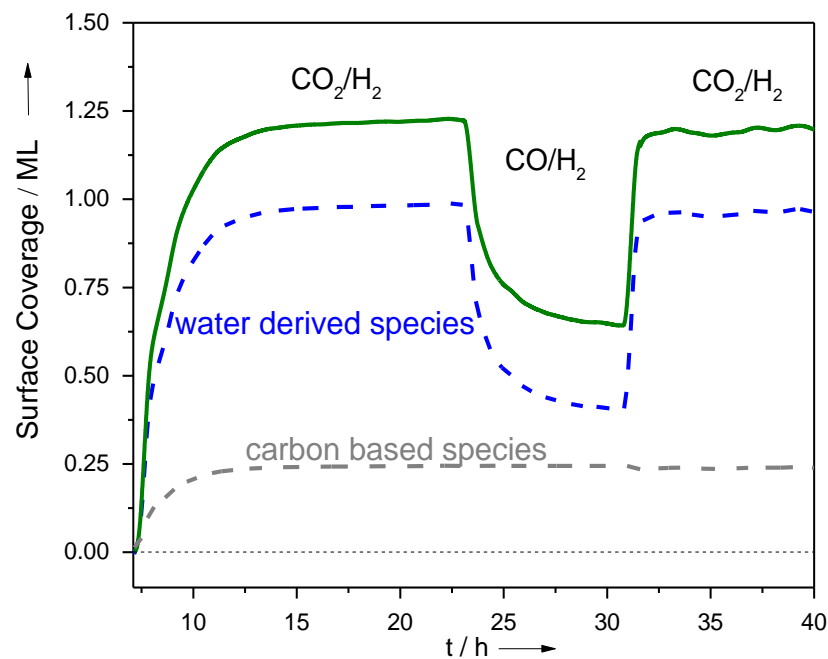
Theoretical mass increase of the catalyst under estimation of **full covered surface** with one type of species

Group/M, g mol^{-1}	Surface stoichiometry	$\Delta M, \%$ (Cu sites)	$\Delta M, \%$ (ZnO sites)	Full $\Delta M, \%$ (Cu/ZnO _x sites)
H ₂ O/18 water	1	0.72	0.49	1.21
OH/17 hydroxy	1	0.68	0.46	1.14
OCH ₃ /31 methoxy	1	1.24	0.85	2.09
CHOO/45 formate	2/1	1.8/0.9	1.2/0.6	3/1.5

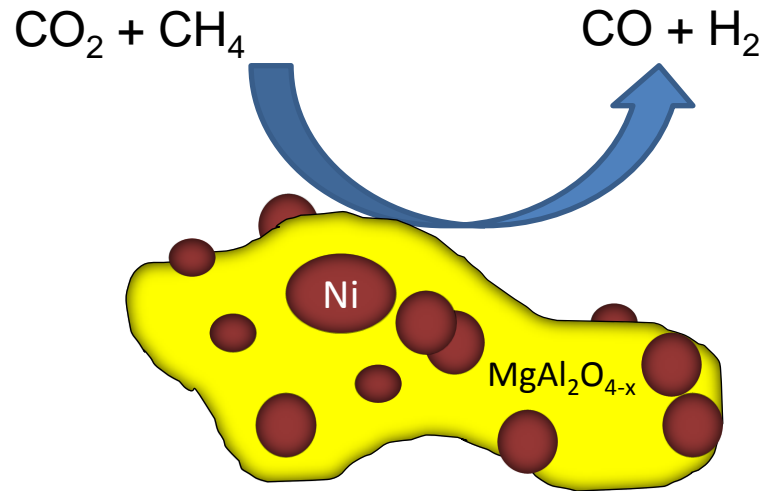
Addition of 1.5% H₂O (250°C, 1bar)



TG Methanol Synthesis (250°C, 30bar)



Case Study: Dry Reforming of methane



Target Reaction Dry reforming (DRM): $\text{CO}_2 + \text{CH}_4 \rightleftharpoons 2 \text{CO} + 2 \text{H}_2$ $\Delta H^0 = 247 \text{ kJ/mol}$

Side reactions (\Rightarrow catalyst deactivation because of **coking**):

- Boudouard reaction: $2 \text{CO} \rightleftharpoons \text{C} + \text{CO}_2$ $\Delta H^0 = -171 \text{ kJ/mol}$
- Methane pyrolysis: $\text{CH}_4 \rightleftharpoons \text{C} + 2 \text{H}_2$ $\Delta H^0 = 75 \text{ kJ/mol}$

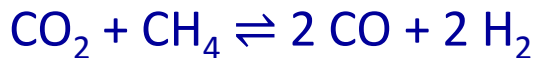
Suppression of side reactions:

- high reaction temperature (900 °C)

\Rightarrow high temperature stable, long term active, non coking materials required

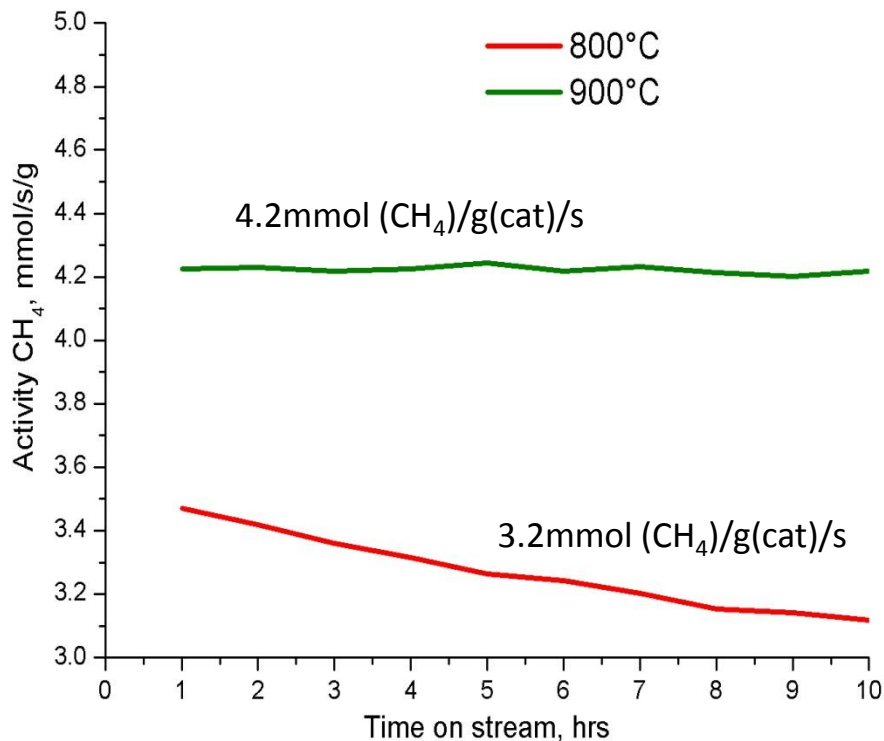
$\Rightarrow \Rightarrow$ Ni/MgAl₂O₄ catalyst

Case Study: Dry Reforming of methane



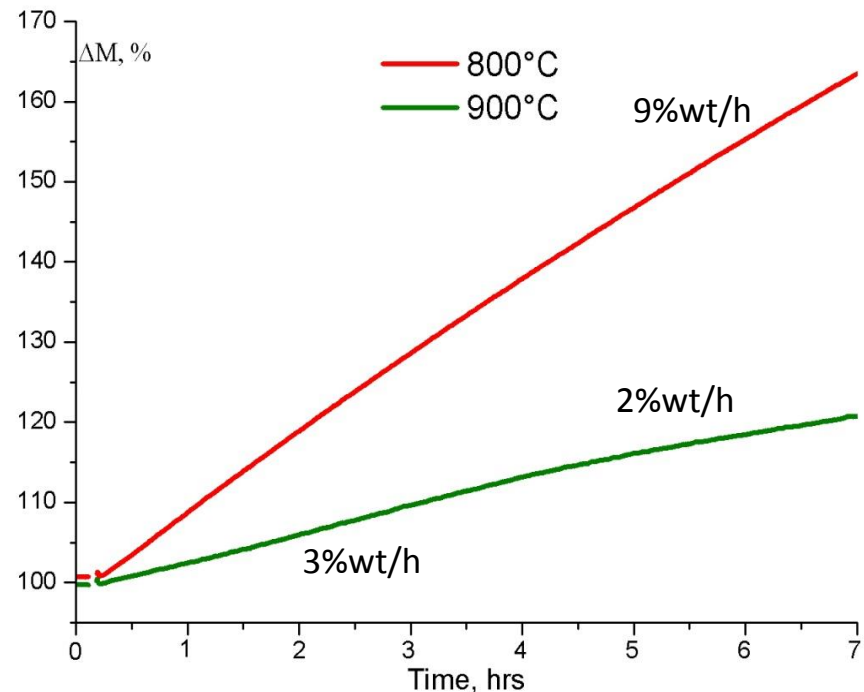
$$\Delta H^0 = 247 \text{ kJ/mol}$$

Activity



- Better performance at higher temperatures

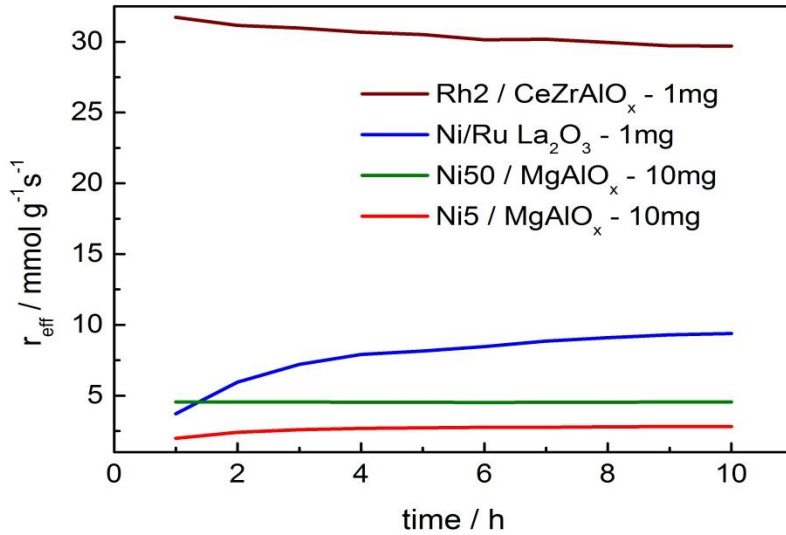
Weight change



- Continuous coke formation

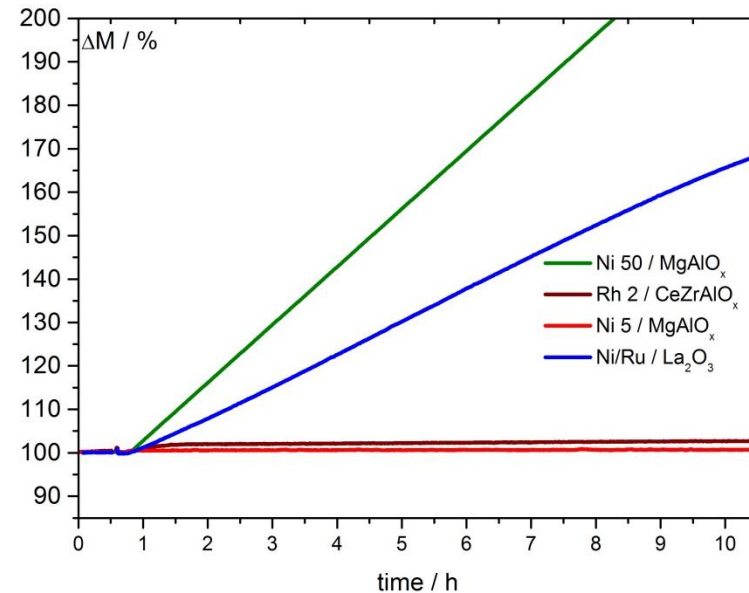
Case Study: Dry Reforming of methane

Activity in DRM



- Continues coking process
- Less coking at lower Ni concentrations

Carbon formation

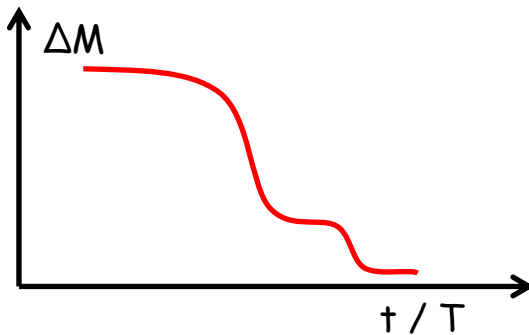


Tarasov et al., Chem. Ing. Tech., **2014**, 86, 1916-1924

Definition of TA

Group of physical-chemical methods which deal with studying materials and processes under conditions of programmed changing's of the surrounding temperature.

Thermogravimetry

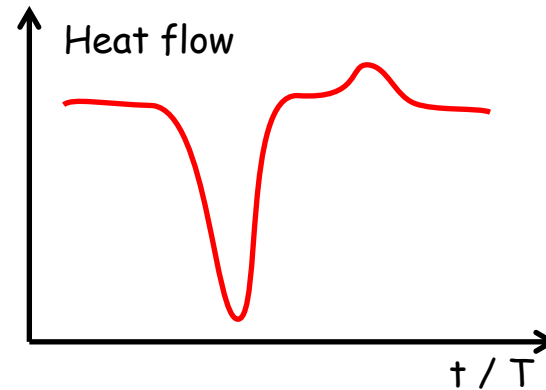


$$r \equiv \frac{dN}{d\tau} = \frac{1}{M} \cdot \frac{dm}{d\tau}$$

$$\Delta m = M \cdot \Delta N$$

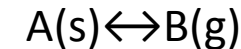
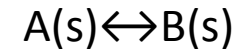


Differential Scanning Calorimetry



$$\phi \equiv \frac{dQ}{d\tau} = m \cdot C_p \cdot \frac{dT}{d\tau}$$

$$\Delta Q = m \cdot C_p \cdot \Delta T$$



Key parameters:

Course of the reaction, yield of the reaction Enthalpy of formation/transformation
(reaction, phase transition)

Differential Scanning Calorimetry (DSC) –

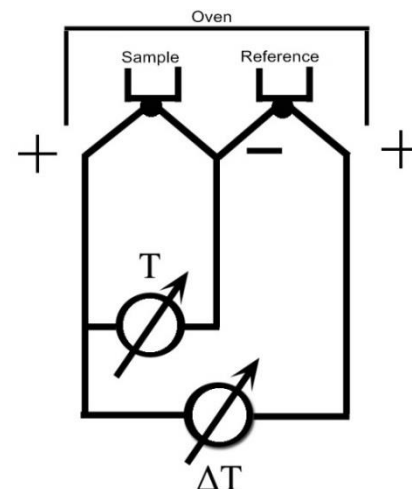
experimental methods for measuring thermal effects (heat evolution and consumption)

- in extended range of temperatures;
- with improved productivity;
- with higher temporal resolution

Differential – permanently compared to reference

Principle of combined thermocouple

Registration the temperature of the object and temperature difference between sample and reference



Differential Scanning Calorimetry (DSC) –

experimental methods for measuring thermal effects
(heat evolution and consumption)

- in extended range of temperatures;
- with improved productivity;
- with higher temporal resolution

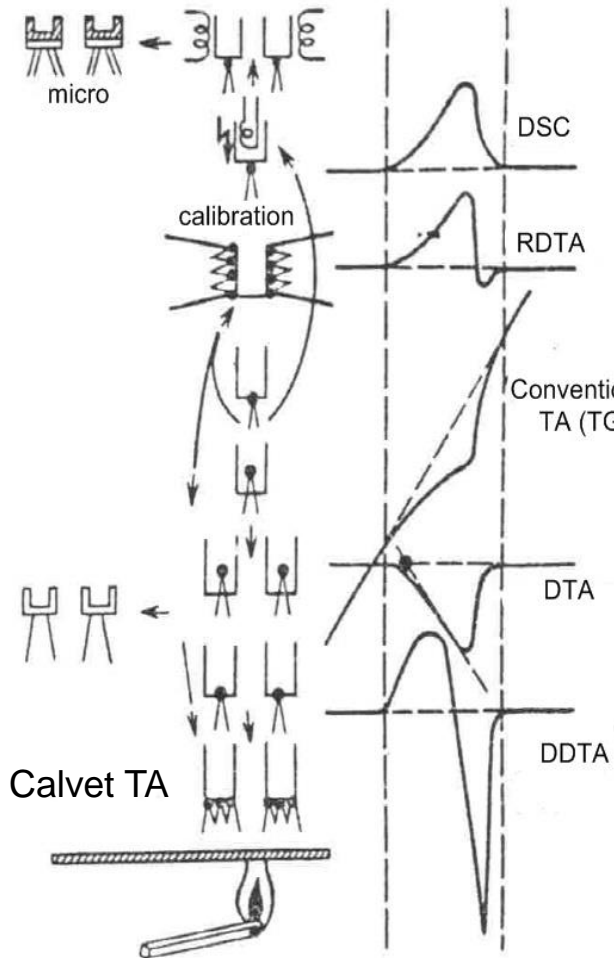
Differential – permanently compared to reference

Scanning – varied (programmed) temperature (permanently and/or stepwise)

Calorimetry – ‘near calorimetric’ (although reduced) precision (typically, 1-2% of measured thermal value) – as a rule satisfactory for a wide range of applications

Based on different technical principles and schemes but fundamentally same physical background: heat transfer and balance

Basic Principles and Terminology



DSC - (Differential Scanning Calorimetry):

Voltage to keep $\Delta T = T_S - T_R = 0$ vs. T

RDTA (Reverse Differential Thermal Analysis) TG

dt/dT vs. T

TA - (Thermal analysis)

T_S vs. t

TG - (Thermogravimetric analysis)

Δm vs. T

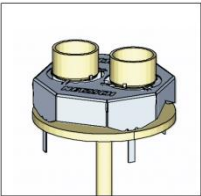
DTA - (Differential Thermal Analysis)

$\Delta T = T_S - T_R$ vs. T

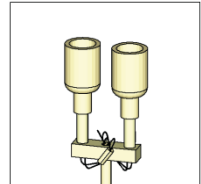
DDTA - (Derivative DTA)

$d\Delta T/dt$ vs. T

DSC-TG



DTA-TG



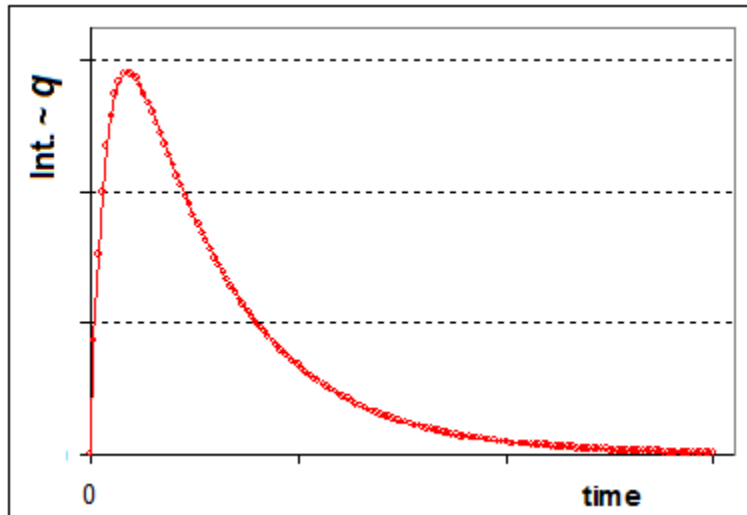
Calvet-DSC



Basic Principles and Terminology

Based on different technical principles and schemes but fundamentally same physical background: heat transfer and balance

$$q = k\Delta T + C(dT/dt) - \text{heat removal and storage}$$



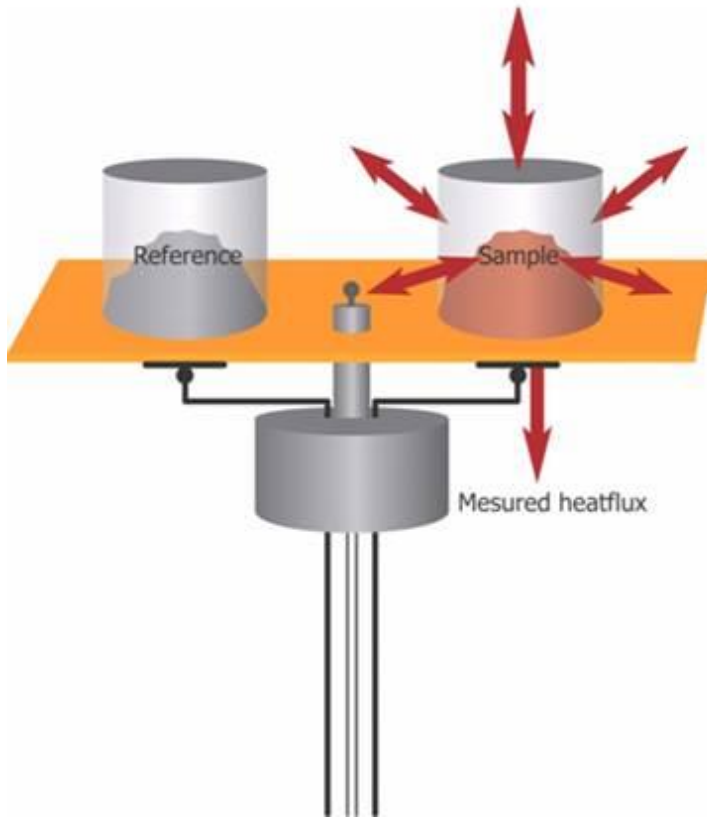
$$Q = \int_0^{\infty} q dt$$

Methods and Instruments

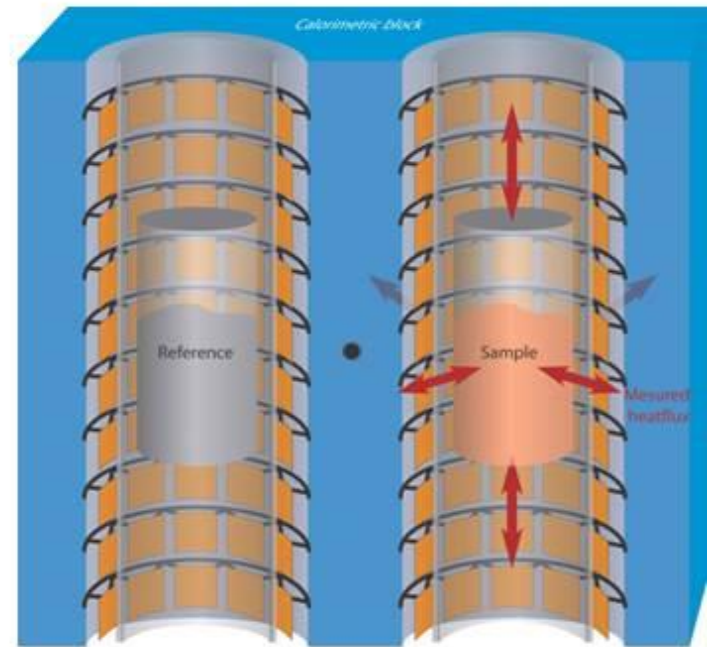
DSC Heat flux

(a)

(b)



Disk shaped, 'Quantitative TA'



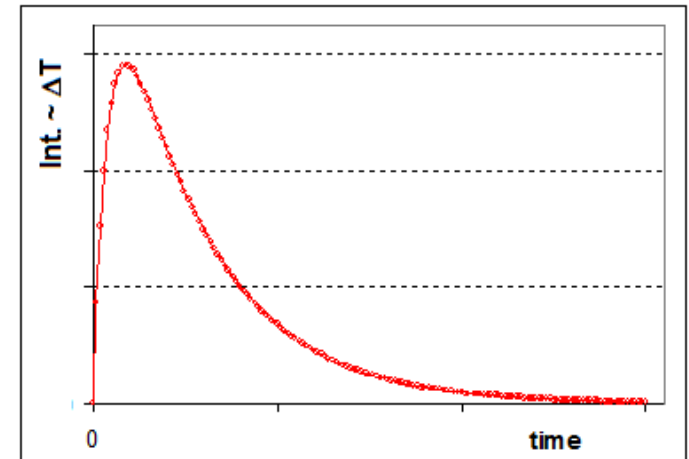
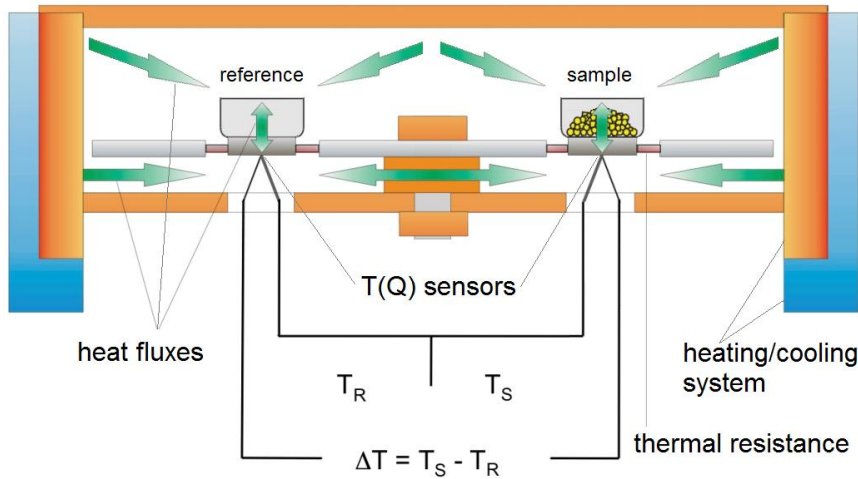
Calvet cell

1. 'Quantitative TA'

- multiple sensors
- tight contact between sensors and holders
- rapid heat removal from the sample

$$C(dT/dt) \approx 0 \text{ and}$$

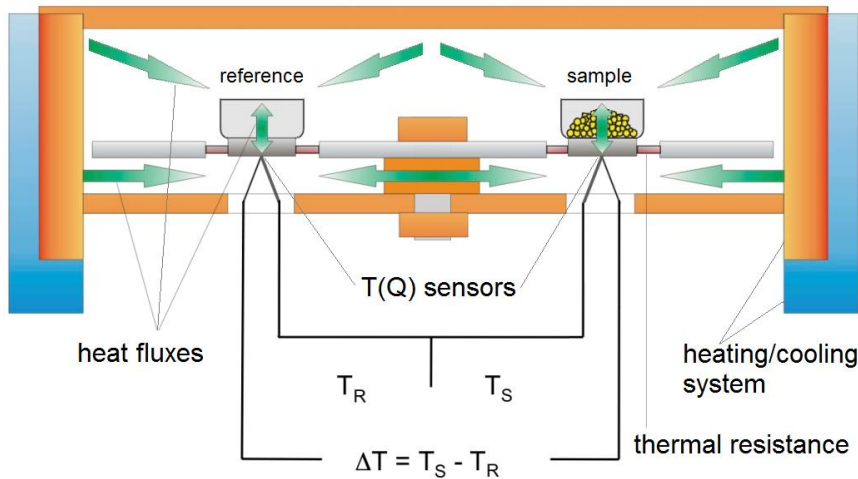
$$q \approx k\Delta T$$



$$Q \approx \int_0^{\infty} \Delta T dt$$

1. 'Quantitative TA'

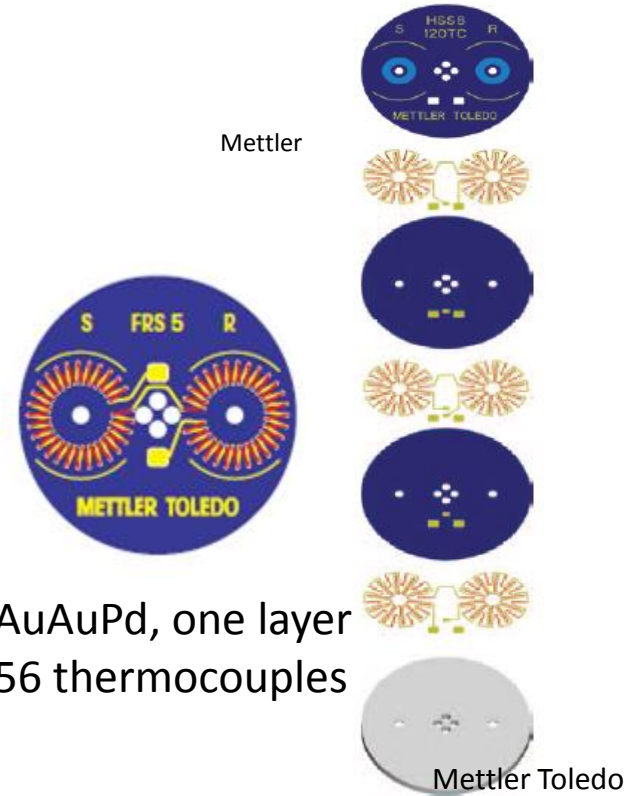
- multiple sensors
- tight contact between sensors and holders
- rapid heat removal from the sample



- relatively simple design;
- wide range of T's;
- compatible with other methods (e.g. TG)
- calibration is critical and can vary from sample to sample;
- gas-solid diffusion

Methods and Instruments

DSC sensors



Methods and Instruments

Thermocouples

Type	Composition	Temperature range, K		Output voltage (0°C), mV
		T _{min}	T _{max}	
T	Cu /constantan	3	670	20
J	Fe/constantan	70	870	34
E	chromel /constantan	-	970	45
K	chromel /alumel	220	1270	41
S	Pt/PtRh (10)	270	1570	13
P	Platinel/AuPd	500	1400	12
C	W/WRe(26)	-	2670	39
N	Nicrosil/Nisil	-	1200	39

Constantan - 58% Cu, 42% Ni

Alumel – 94% Ni, 2% Al, 1,5% Si, 2,5 % Mn

Platinel – 55% Pd, 31% Pt, 14% Au

Chromel – 89% Ni, 10% Cr, 1%Fe

Nicrosil/Nisil – Ni, Cr, Silicon/Ni, Silicon



Cu/Constantan disk sensor on Si(X) wafer.

μ sensor



CuNi disk sensor on Ag plate.

τ sensor



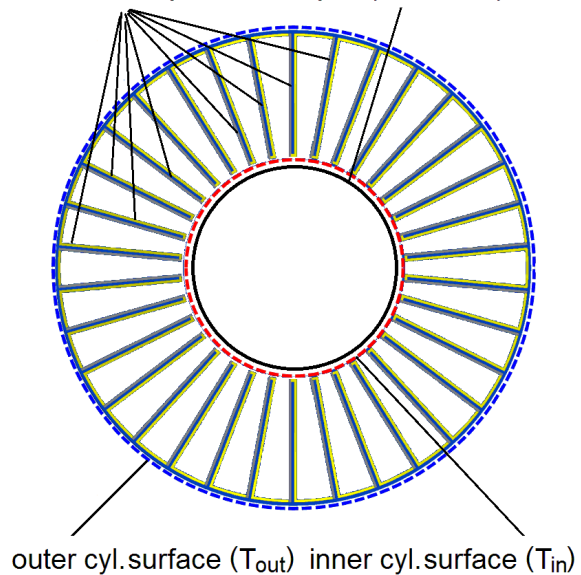
Pt-PtRh(10) diskshaped thermocouple

2. 'Heat-flux', or 'heat-conductive', or Calvet-type DSC

- heat flux is measured outside of the sample assuming that it is proportional to the ΔT on different distances from it

Calvet sensor (top view)

thermocouple sample (reaction) tube



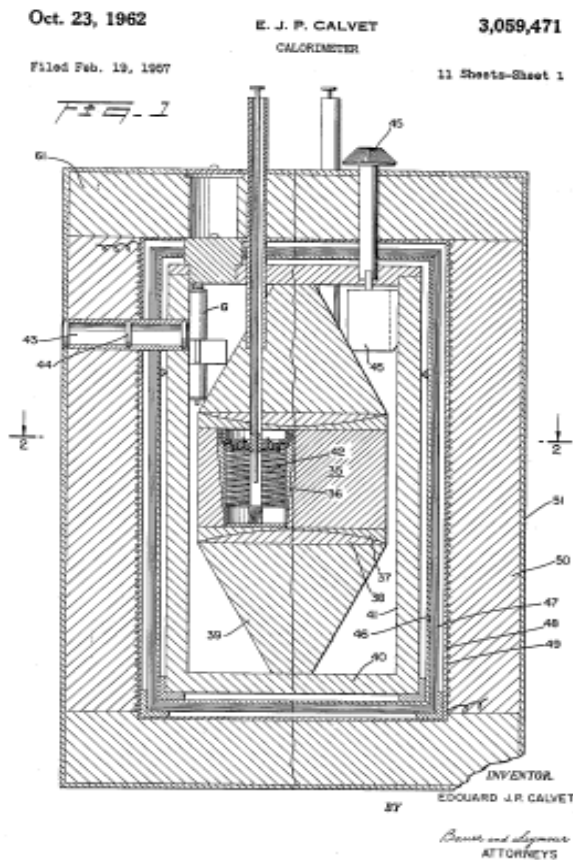
$$q \sim (T_{in} - T_{out})$$

Calvet calorimetry (incl. DSC):

- none of the TC's measures the temperature of the sample (!!!);
- the DSC signal is formed as ΔT between two cylindrical surfaces (inner and outer) on different distances from the sample

2. 'Heat-flux', or 'heat-conductive', or Calvet-type DSC

- heat flux is measured outside of the sample assuming that it is proportional to the ΔT on different distances from it



Oct. 23, 1962

E. J. P. CALVET
CALORIMETER

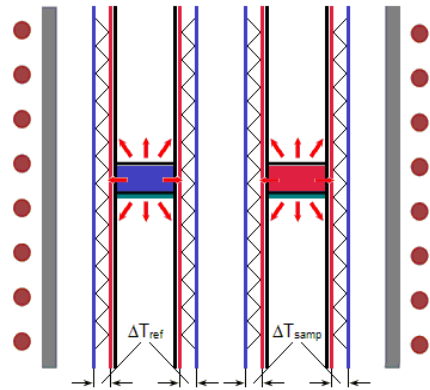
3,059,471

Filed Feb. 19, 1967

11 Sheets-Sheet 1

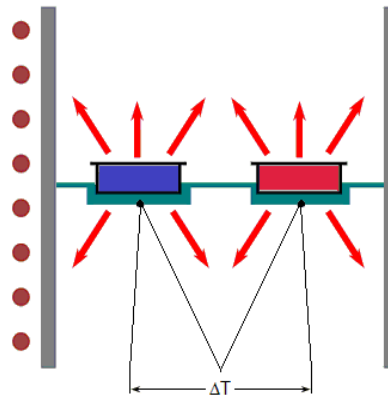
Side view: Calvet (3D) vs. TA (2D) sensing

3D



$$q_{\text{diff}}^{3D} \sim (\Delta T_{\text{samp}} - \Delta T_{\text{ref}})$$

2D

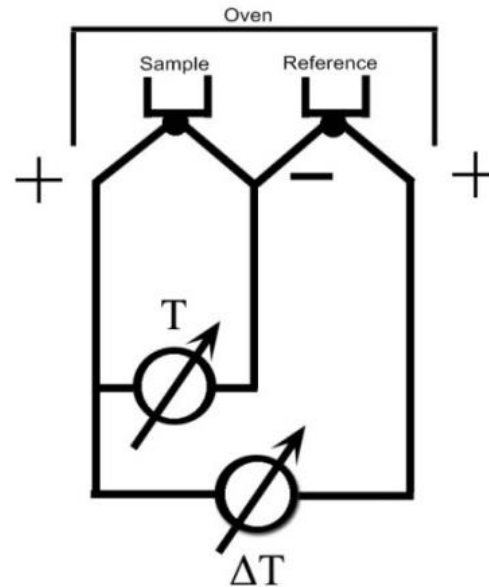


$$q_{\text{diff}}^{2D} \sim \Delta T$$

the sample does not play the role of 'thermal resistance';

- no tight contact between sample (and reference) holder(s) and the sensor is required;
- 3D heat sensing;
- good gas-solid mass-transfer conditions;
- high compatibility (e.g. with TGA)
- relatively low temporal resolution

3D vs. 2D sensing: more efficient (complete) capturing of heat fluxes from/to the sample – lower sensitivity to the sample properties !!!



$$q = K \cdot \Delta T + C \cdot \frac{\partial T}{\partial t} \approx K \left[\Delta T + \tau \left(\frac{d\Delta T}{dt} \right) \right] - \text{Tian equation}$$

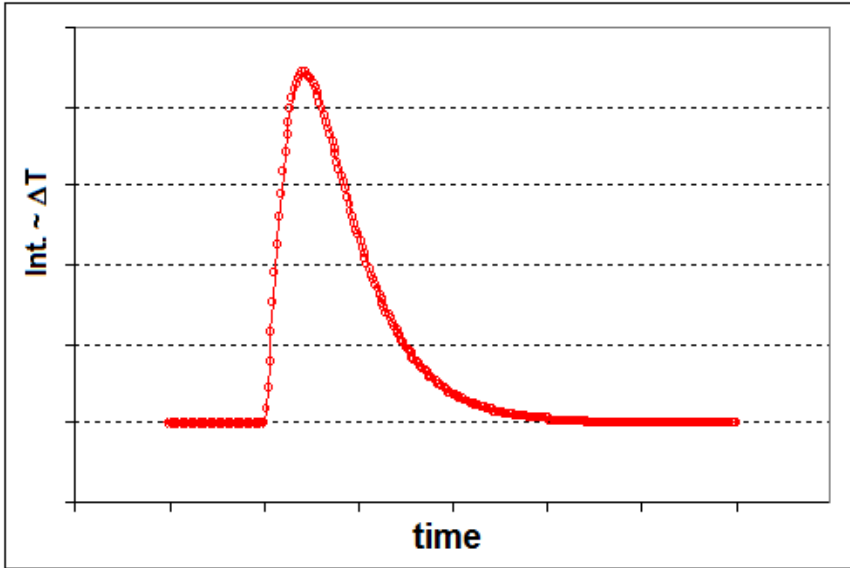
heat removal and storage

q – heat flux at every moment of time

K – specific thermal conductivity

C – specific thermal capacity

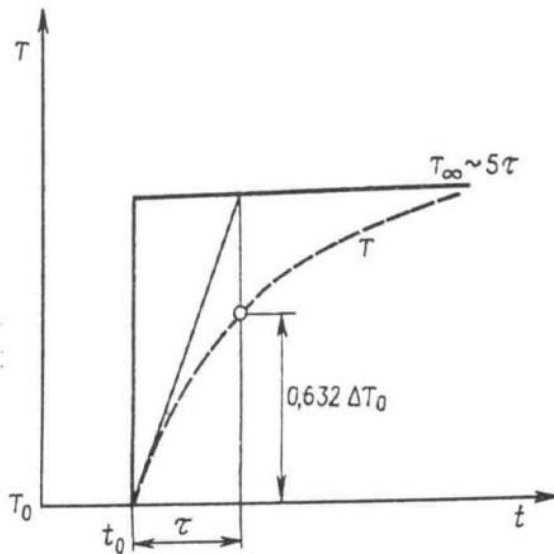
τ – K/C characteristic time constant



$$Q = \int_0^{\infty} q dt \approx a \int_0^{\infty} \Delta T dt$$

$$q = k\Delta T + C(dT/dt) \approx k\Delta T + C(d\Delta T/dt) = k[\Delta T + \tau^*(d\Delta T/dt)]$$

$$\tau^* = C/k - \text{time constant of fluxmeter}$$

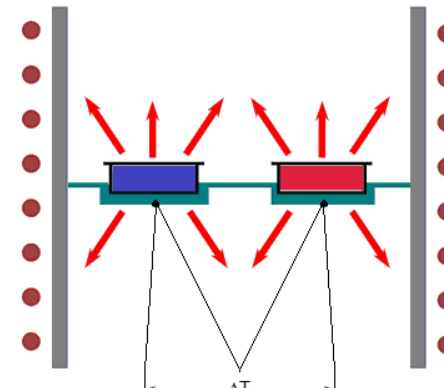
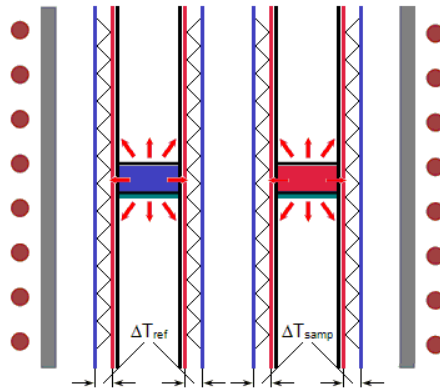


Time constant is depended on design, construction and materials of the calorimetric cell.

Side view: Calvet (3D) vs. TA (2D) sensing

3D

2D



$$q = k[\Delta T + \tau^*(d\Delta T/dt)]$$

$$q_{diff}^{3D} \sim (\Delta T_{samp} - \Delta T_{ref})$$

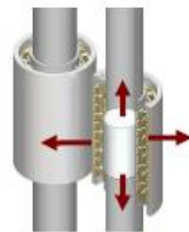
$$q_{diff}^{2D} \sim \Delta T$$

$$k \downarrow \Rightarrow \tau^* (\approx C/k) \uparrow$$

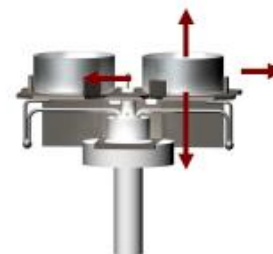
$$k \uparrow \Rightarrow \tau^* (\approx C/k) \downarrow$$

$$\langle q \rangle \uparrow @ \tau^* \uparrow$$

$$\langle q \rangle \downarrow @ \tau^* \downarrow$$



Example of 3D calorimetric sensor



Example of plate-shape DSC sensor (2D)

All Heat convection, conduction and radiation is measured

Only heat conducted directly through the bottom of the vessel is measured

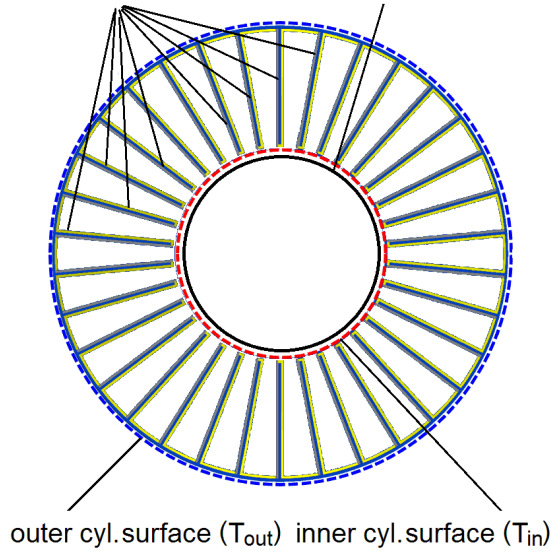
Three ranges of characteristic times of the process should be considered:

$\tau_{\theta} < 0.1 \tau$ Thermal inertia of the registration system completely shades the kinetics

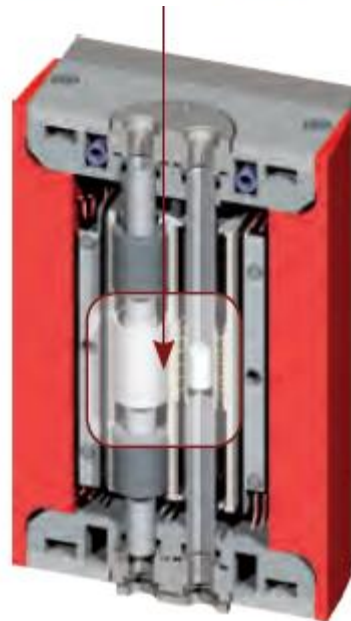
$\tau_{\theta} > \tau$ When the kinetics may rather accurately be determined using Tian equation

$0.1 \tau < \tau_{\theta} < \tau$ When the available methods give kinetics that is somewhat distorted by the thermal inertia of a sample

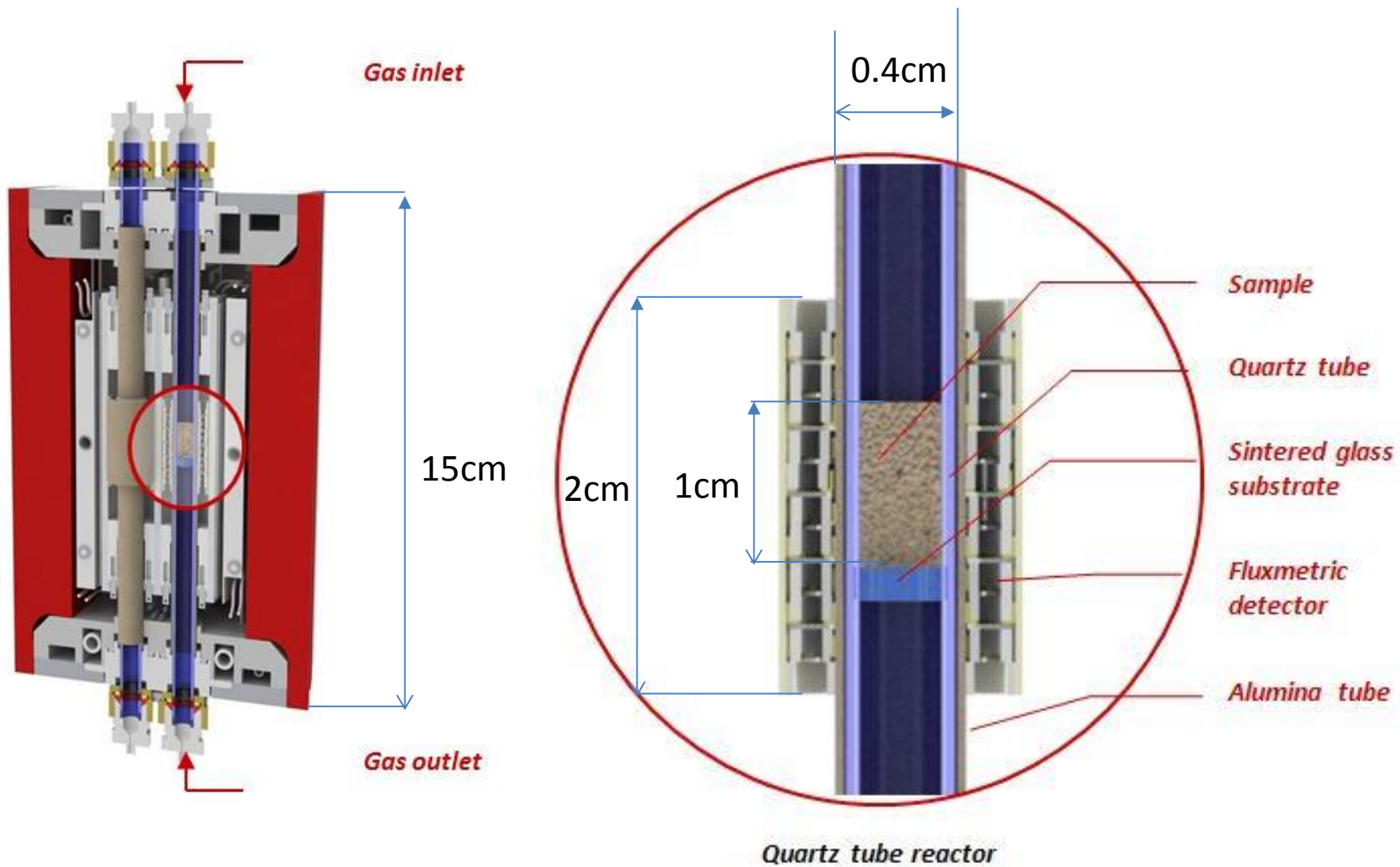
Calvet sensor (top view)
thermocouple sample (reaction) tube

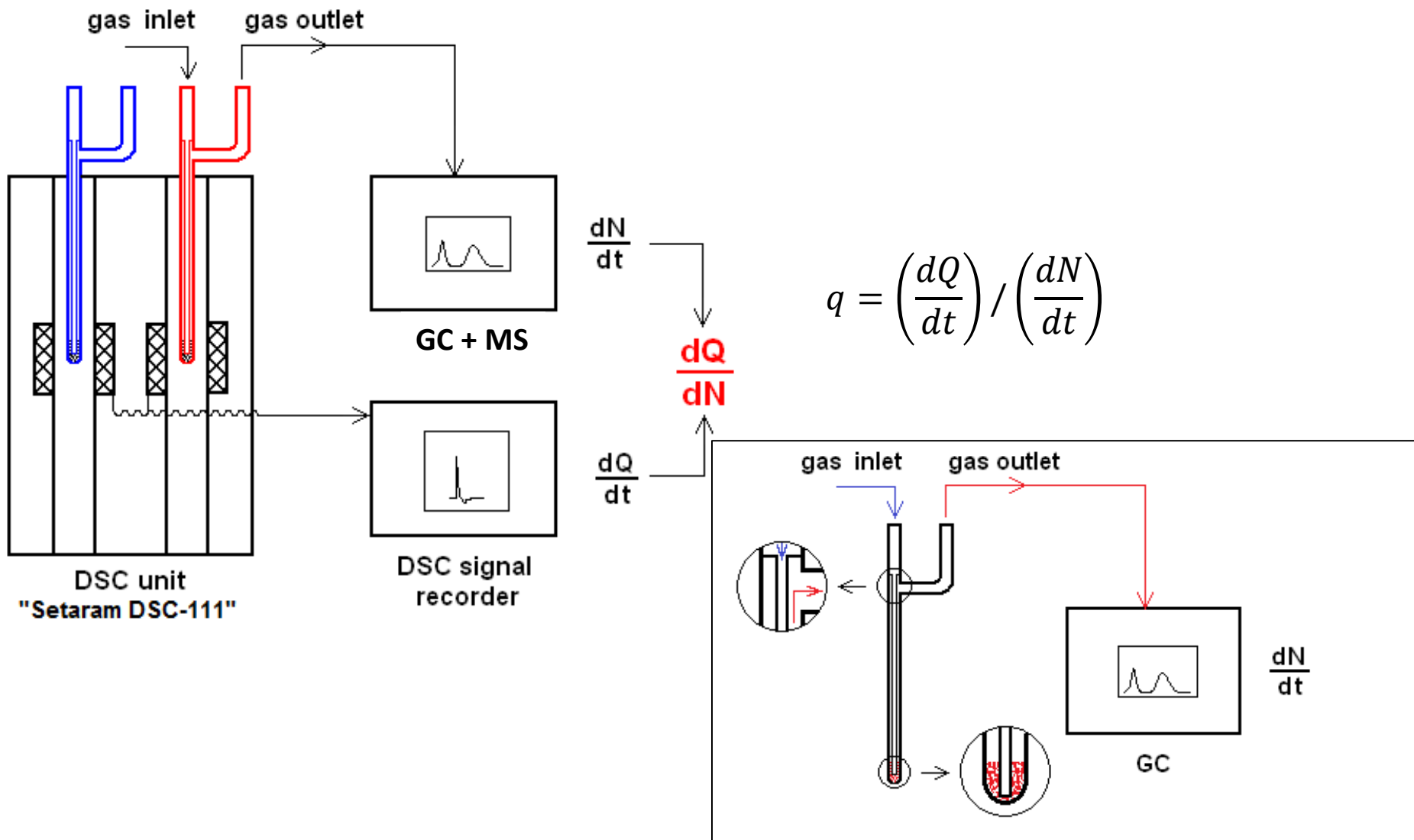


$$q \sim (T_{in} - T_{out})$$



In-situ DSC setup

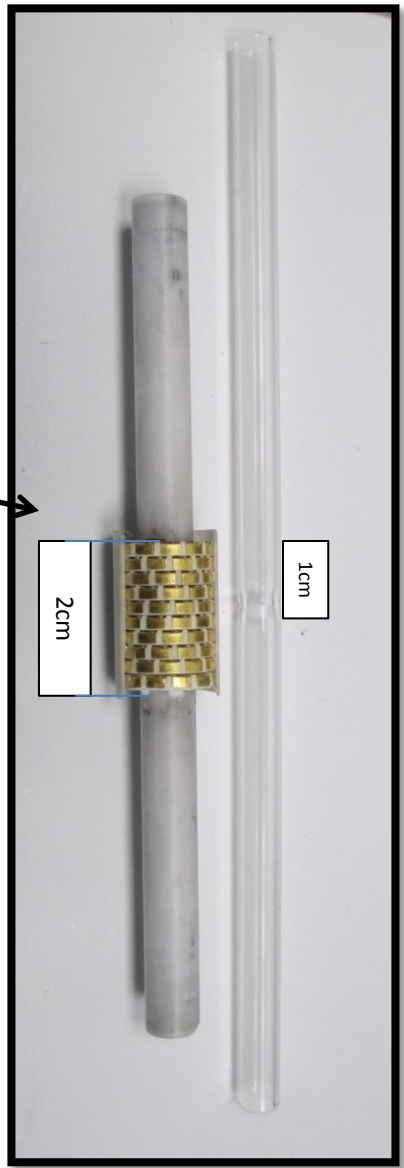
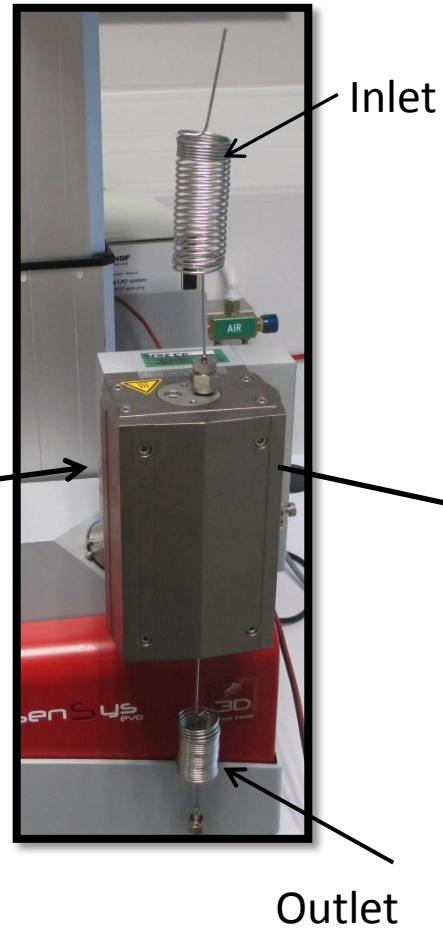




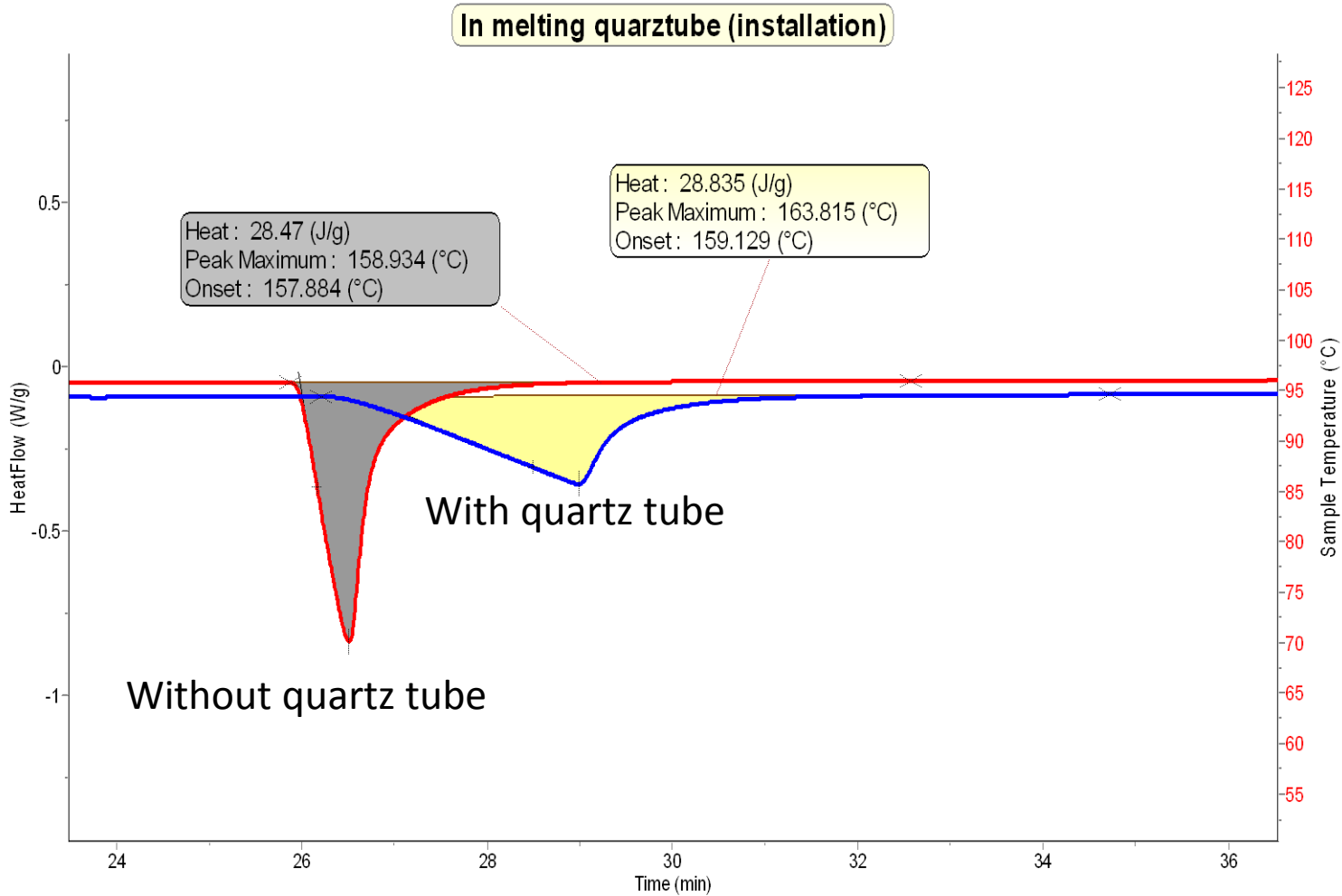
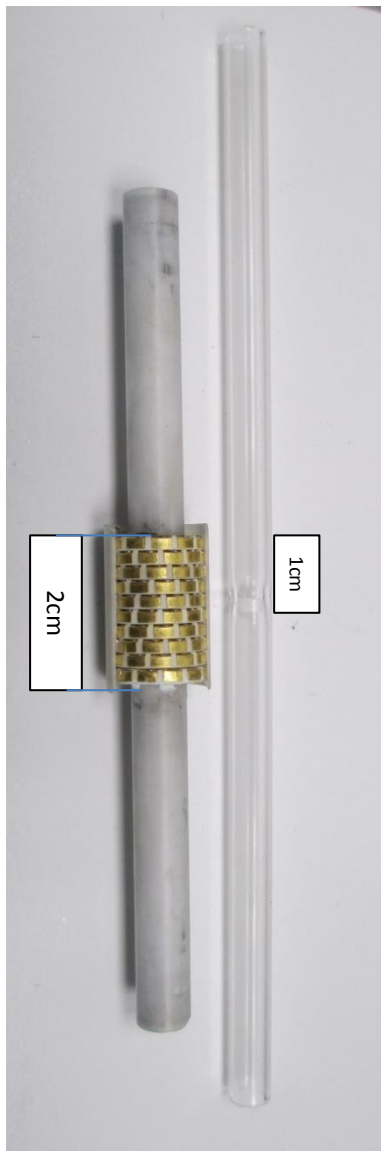
Sinev et al.

In-situ DSC setup

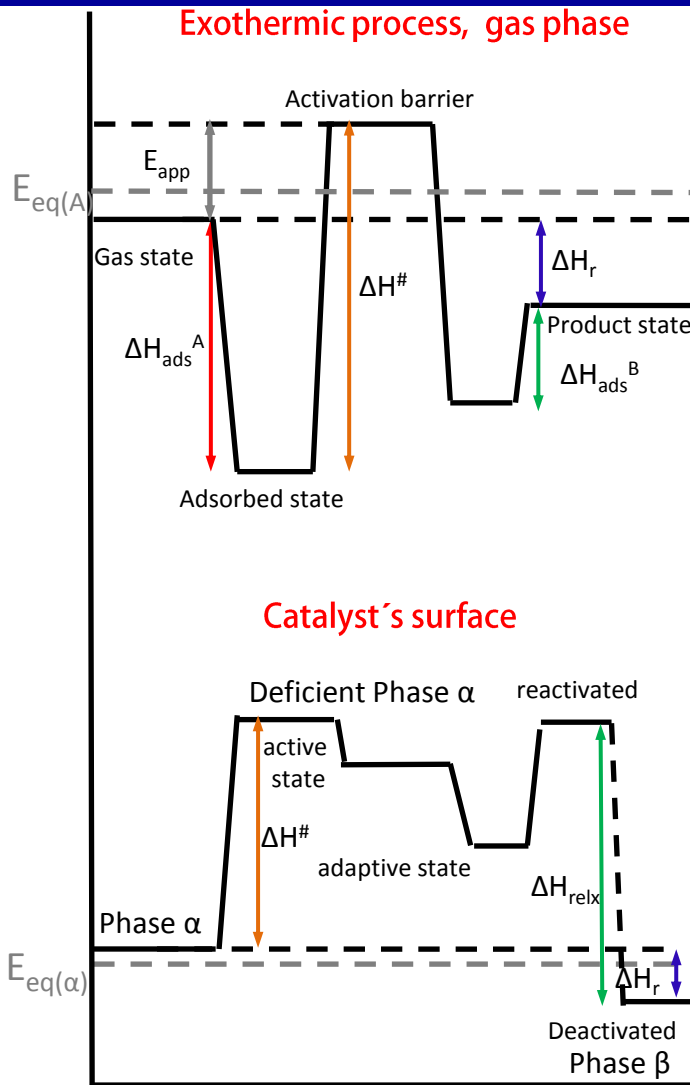
MAX-PLANCK-GESELLSCHAFT



In-situ DSC setup



What can we measure?



Simplified schematic representation

Transformation of gas phase molecules

- Information on reaction kinetics (E_a)
- Simulation of different conditions in-situ
- Adsorption - desorption enthalpies

Transformation in solid state

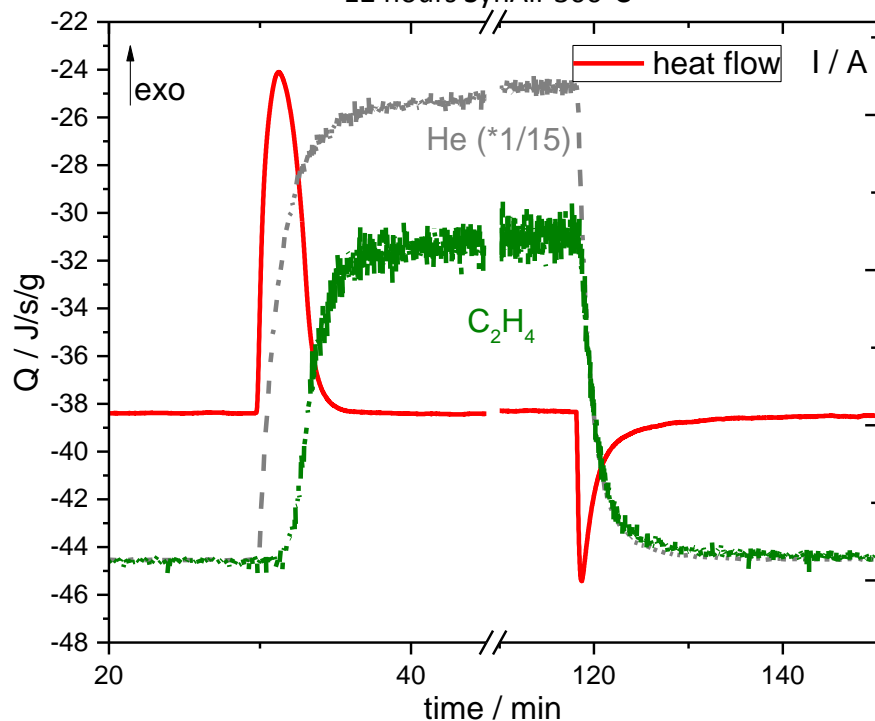
- Redox dynamics
- Effects of oxygen diffusion into subsurface
- Redistribution of bulk and surface oxygen
- Oxygen binding energy (oxides)
- Thermochemistry of defects formation

Adapted using: van Santen, R. A., *Modern Heterogeneous Catalysis*, Wiley, 2017
and Schlögl, R., *Introduction to Heterogeneous Catalysis, Lecture*, FHI Berlin, 2017

5%Ag/SiO₂, Max Lamoth

In-situ DSC

30°C, total flow 30mlm, P_{total} 1,15bar
12 hours SynAir 300°C



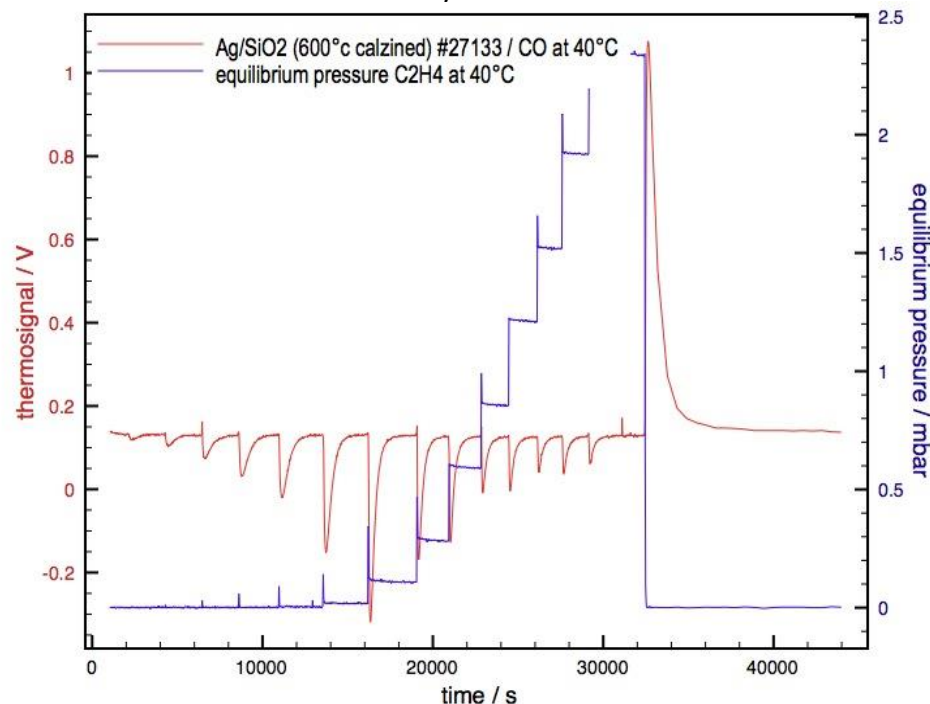
$$\Delta H_{\text{ads}} = -94 \text{ kJ/mol}(\text{C}_2\text{H}_4)$$

$$N(\text{C}_2\text{H}_4) = 26 \mu\text{mol/g}(\text{cat})$$

reversible

Microcalo

40°C, Prange 0-3mbar
3 hours SynAir 300°C



$$\Delta H_{\text{ads}} = -87-33 \text{ kJ/mol}(\text{C}_2\text{H}_4)$$

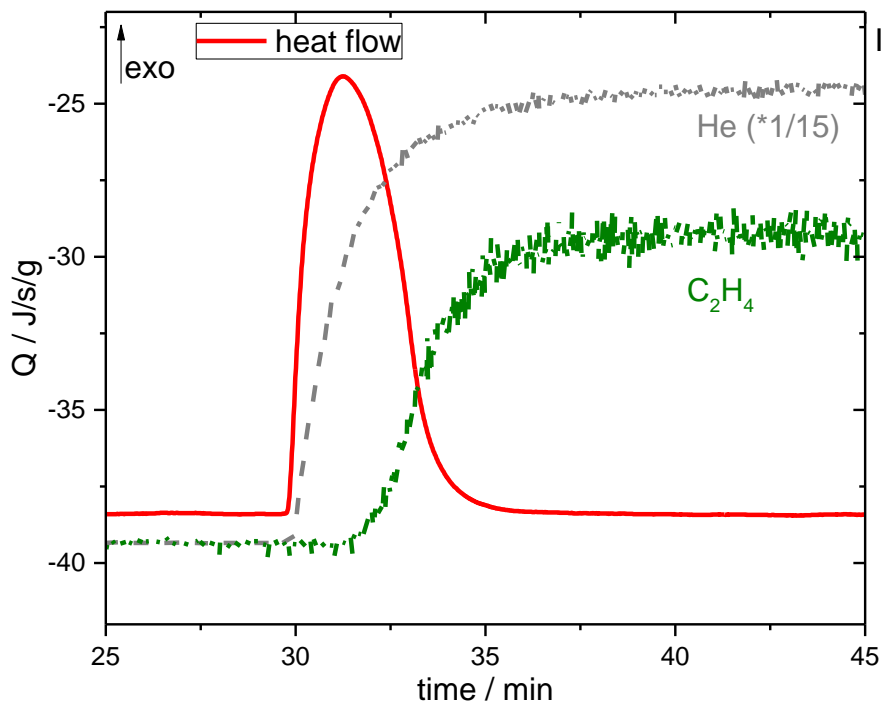
$$N(\text{C}_2\text{H}_4) = 33 \mu\text{mol/g}(\text{cat})$$

reversible

5%Ag/SiO₂, Max Lamoth

In-situ DSC

30°C, total flow 30mlm, P_{total} 1.15bar, P_{C₂H₄} 0.6mbar
12 hours SynAir 300°C



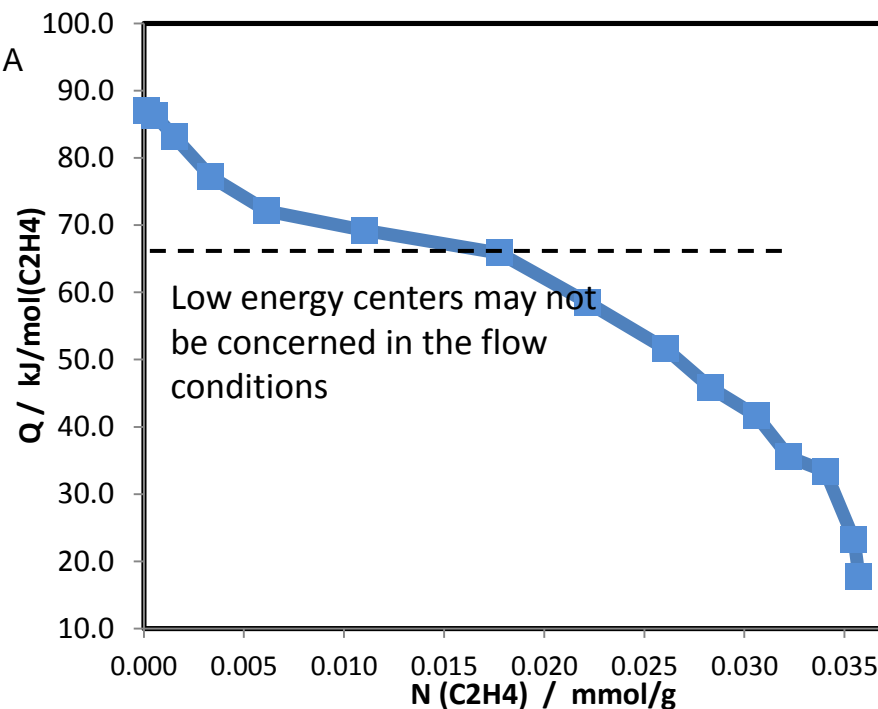
$$\Delta H_{\text{ads}} = -94 \text{ kJ/mol(C}_2\text{H}_4)$$

$$N(\text{C}_2\text{H}_4) = 26 \mu\text{mol/g(cat)}$$

reversible

Microcalo

40°C, Prange 0-3mbar
3 hours SynAir 300°C



$$\Delta H_{\text{ads}} = -87-33 \text{ kJ/mol(C}_2\text{H}_4)$$

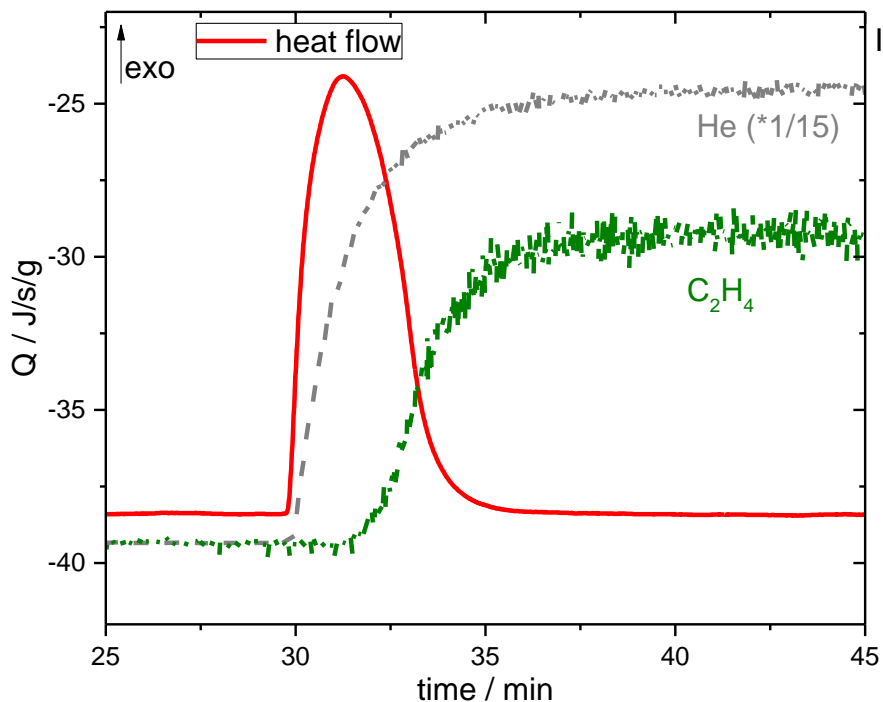
$$N(\text{C}_2\text{H}_4) = 33 \mu\text{mol/g(cat)}$$

reversible

5%Ag/SiO₂, Max Lamoth

In-situ DSC

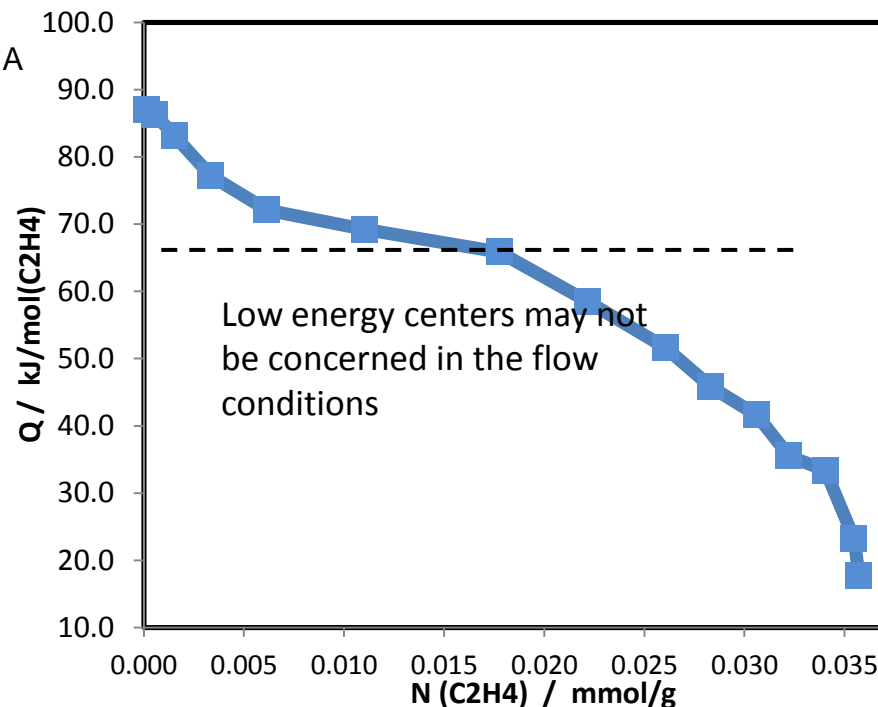
30°C, total flow 30mlm, P_{total} 1.15bar, P_{C₂H₄} 0.6mbar
12 hours SynAir 300°C



Desorption and readsorption are occurring simultaneously with diffusion

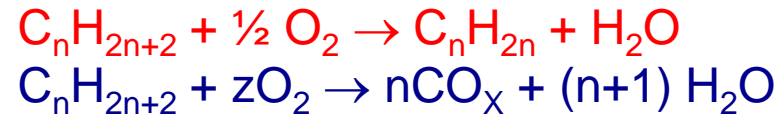
Microcalo

40°C, Prange 0-3mbar
3 hours SynAir 300°C



In UHV systems diffusion takes part in a very limited extent, while readsorption can be avoided using sufficiently high pumping speed

Case study: alkane ODH over VSb/Al₂O₃

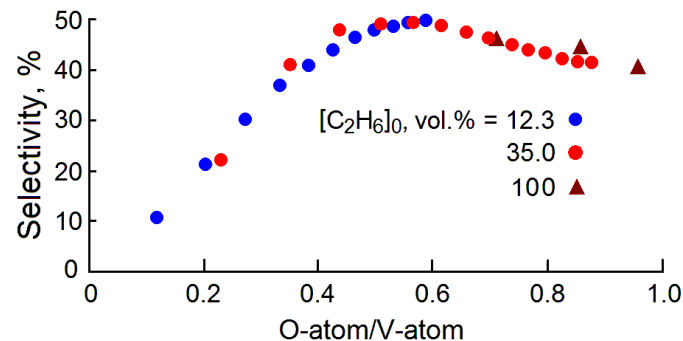
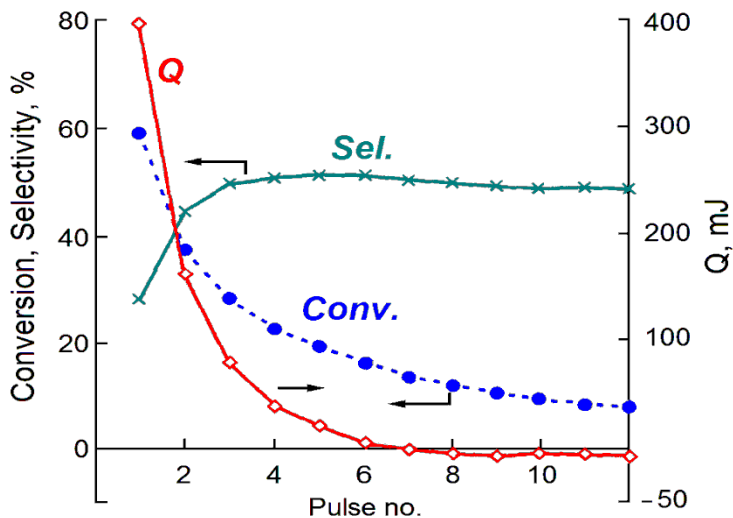
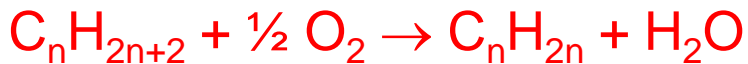


Catalysts – V-containing bulk and supported oxides

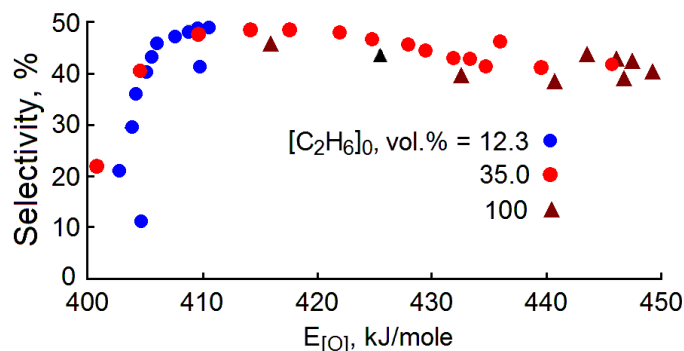
'Classical' Red-Ox Kinetics over V-containing catalysts –
Mars-van-Krevelen* or oxygen rebound-replenish (ORR) mechanism



Sinev et al.



V(4+) state is optimal for high selectivity to ethylene

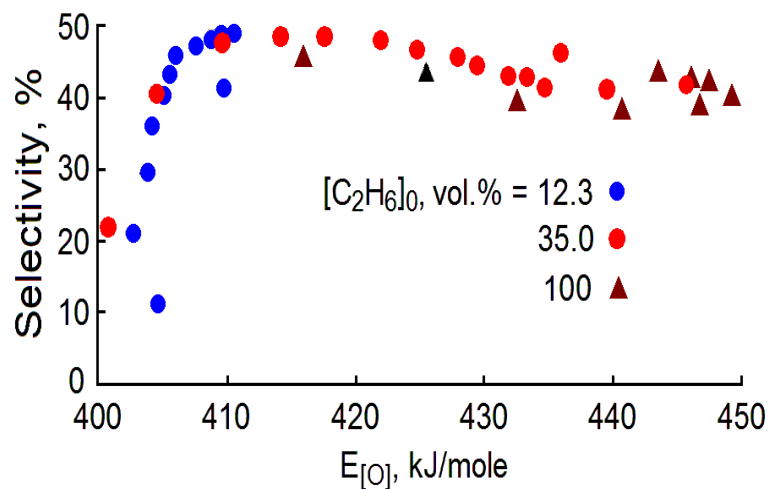


V(5) → V(4+) – jump of S @ small variations of E_[O];

V(4+) → (V3+) – slow decrease of S in a wide range of E_[O] variation

🔑 ‘Chemical’ factor (i.e. state of surface sites and their interaction with HC’s) is more important than ‘energy’ one

Sinev et al.

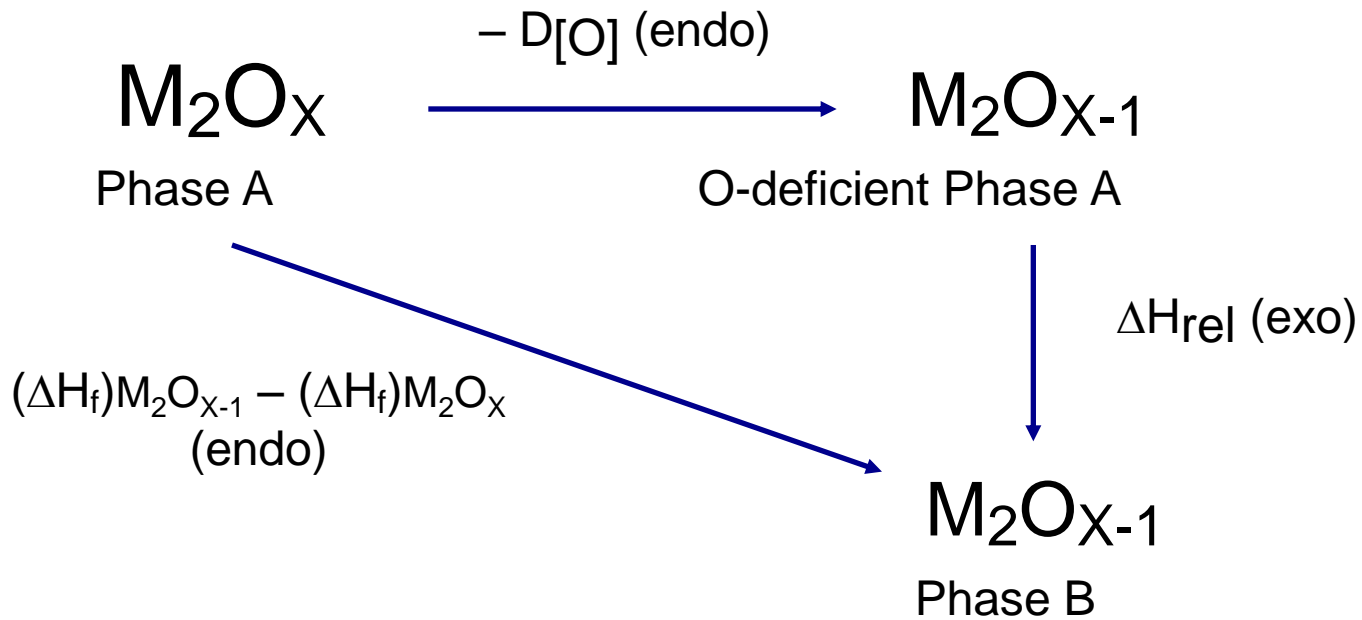


$$(\Delta H_f)_{M_2O_{x-1}} - (\Delta H_f)_{M_2O_x} \approx E_{[O]}$$



Is $E_{[O]} \approx (\Delta H_f)_{M_2O_{x-1}} - (\Delta H_f)_{M_2O_x} ???$

Sinev et al.



$D_{[O]}$ – O-binding energy (in ‘phase homogeneity’ range);

$(\Delta H_f)_{M_2O_x}$, $(\Delta H_f)_{M_2O_{x-1}}$ – standard (tabulated) values;

ΔH_{rel} – enthalpy of relaxation (elimination of vacancies, lattice re-organization, etc.)

$$|(\Delta H_f)_{M_2O_{x-1}} - (\Delta H_f)_{M_2O_x}| < |E_{[O]}| < |D_{[O]}|$$

Sinev et al.

Experimentally measured value